mathematics

MDPI

Review

A Review of Theories and Numerical Methods in Nanomechanics for the Analysis of Nanostructures

Mostafa Sadeghian *, Arvydas Palevicius * and Giedrius Janusas

Faculty of Mechanical Engineering and Design, Kaunas University of Technology, Studentu 56, 51424 Kaunas, Lithuania

* Correspondence: mostafa.sadeghian@ktu.edu (M.S.); arvydas.palevicius@ktu.lt (A.P.)

Abstract

Nanostructures, such as carbon nanotubes (CNTs), graphene, nanoplates, etc., show behaviors that classical continuum theories cannot capture. At the nanoscale, size effects, surface stresses, and nonlocal interactions become important, so new models are needed to study nanostructures. The main nanomechanics theories that are used in recently published papers include nonlocal elasticity theory (NET), couple stress theory (CST), and nonlocal strain gradient theories (NSGTs). To solve these models, methods such as finite elements, isogeometric analysis, mesh-free approaches, molecular dynamics (MD), etc., are used. Also, this review categorizes and summarizes the major theories and numerical methods used in nanomechanics for the analysis of nanostructures in recently published papers. Recently, machine learning methods have enabled faster and more accurate prediction of nanoscale behaviors, offering efficient alternatives to traditional methods. Studying these theories, numerical models and data driven approaches provide an important foundation for future research and the design of next generation nanomaterials and devices.

Keywords: nanomechanics theories; numerical methods; nanostructures; machine learning; review

MSC: 74G60; 74H45; 74S99; 74A99

check for updates

Academic Editor: Vasily Novozhilov

Received: 9 October 2025
Revised: 31 October 2025
Accepted: 10 November 2025
Published: 12 November 2025

Citation: Sadeghian, M.; Palevicius, A.; Janusas, G. A Review of Theories and Numerical Methods in Nanomechanics for the Analysis of Nanostructures. *Mathematics* **2025**, *13*, 3626. https://doi.org/10.3390/math13223626

1. Introduction

Nanomechanics is a rapidly developing field that deals with the mechanical behavior of materials and structures at the nanometer scale. Unlike classical mechanics (which assumes a continuum medium without internal length scales), nanomechanics consider phenomena such as interatomic interactions, surface stresses, and discrete lattice effects that become dominant when the characteristic dimension of a structure approaches a few nanometers. Typical nanostructures include CNTs, graphene sheets, nanowires, nanoplates, thin films, and components of micro/nanoelectromechanical systems (MEMS/NEMS). These systems are widely used in electronics, sensors, actuators, biomedical devices, and energy-harvesting technologies [1–3].

At the nanoscale, conventional continuum theories fail to accurately predict the mechanical response of materials. This limitation arises from several fundamental challenges. First, size effects play a critical role. Experimental studies have demonstrated that nanostructures may exhibit stiffening or softening as their characteristic dimensions decrease, a phenomenon that classical elasticity cannot capture. Second, surface effects become dominant due to the extremely high surface-to-volume ratio at the nanoscale. As a result, surface

stress and interface energy contribute significantly to the overall mechanical behavior of nanostructures. Finally, in some cases (particularly in ultra-thin films, nanowires, and quantum dots), quantum effects cannot be neglected. Interactions among electronic states and lattice vibrations modify the mechanical response that demands quantum-informed or multiscale models [3,4].

To address these limitations, researchers have extended classical continuum mechanics by incorporating intrinsic length scales, surface elasticity, and nonlocal interactions. The NET proposed by Eringen [5] introduces the concept that stress at a material point depends not only on local strain but also on strains in its neighborhood, making it suitable for wave propagation and vibration analysis in nanostructures. Subsequently, strain gradient theories (Mindlin [6]; Fleck and Hutchinson [7]) included higher-order gradients of strain in the energy functional, enabling the capture of size-dependent hardening. Similarly, CST and its modified versions incorporated internal length parameters through rotational effects and bending moments [8,9]. To account for dominant surface contributions, the Gurtin–Murdoch surface elasticity theory [10] provided a continuum framework, including interface energy. For fracture and discontinuities, the peridynamics theory introduced by Silling [11] reformulated mechanics in an integral, nonlocal framework free from spatial derivatives. Similar to these continuum models, atomistic-to-continuum approaches, such as the Cauchy Born rule [12] and quasicontinuum (QC) methods [13], established connections between atomistic simulations (MD, DFT) and continuum models.

In recent years, several review papers have been published about nanomechanics. For example, Barretta et al. [14] reviewed recent progress in nonlocal elasticity for nanostructures, emphasizing the limitations of classical continuum mechanics and the need for scale-dependent models. Eltaher et al. [15] reviewed the research on nonlocal elastic models for nanoscale beams, with a focus on bending, buckling, vibration, and wave propagation analyses. They discussed how classical continuum mechanics fail at small scales and highlighted the effectiveness of Eringen's NET in capturing size-dependent behaviors. Thai et al. [16] presented a review of continuum mechanics models that had been developed to capture size effects in beams and plates. Farajpour et al. [17] reviewed the mechanics of nanostructures such as nanorods, nanobeams, nanoplates, and nanoshells. They explained that experimental studies and MD simulations were difficult and costly, so modified continuum theories have been widely used. Ghayesh and Farajpour [18] reviewed functionally graded (FG) nanoscale and microscale structures. They described how material properties could vary to enhance the performance of MEMS and NEMS devices. The paper summarized findings on vibration, buckling, and deformation of FG beams and plates and pointed toward future applications. Nuhu and Safaei [19] carried out a comprehensive review on the vibration analyses of small-scale structures using nonclassical continuum elasticity theories. Khaniki et al. [20] reviewed the statics and dynamics of electrically actuated nano- and micro-structures. The authors summarized both electrostatic and electrodynamic analyses of beams, plates, and shells, and demonstrated how theoretical models had evolved to include electro-mechanical coupling. They also discussed the applications of such systems in resonators, biosensors, detectors, and diagnostic devices, showing how modeling accuracy had been essential for real-world progress. Yee and Ghayesh [21] presented a review on the bending, buckling, and dynamics of graphene nanoplatelet (GPL)-reinforced structures. They noted that GPL had become an attractive nanofiller because of its low cost and ease of production compared to graphene or carbon nanotubes. Roudbari et al. [4] reviewed size-dependent continuum mechanics models for micro/nanostructures. They examined how nonlocal elasticity, modified couple stress, strain gradient, and micromorphic theories had been employed to study bending, vibration, buckling, and wave propagation in rods, beams, plates, and shells.

Imani Yengejeh et al. [22] reviewed advances in the mechanical analysis of structurally and atomically modified carbon nanotubes. The authors discussed both experimental and computational research, including MD and finite element approaches, which showed how defects reduced stiffness, strength, and vibrational response. They concluded that imperfections significantly influenced the mechanical performance of CNTs and that more realistic models were needed for engineering applications. Soni et al. [23] presented an extensive review of FG carbon nanotube-reinforced composite structures. They summarized studies on the mechanical, thermal, thermo-mechanical, vibrational, and impact responses of beams, plates, shells, and panels reinforced with CNTs. Sayyad et al. [24] reviewed the mechanics of FG nanobeams, focusing on nonlocal continuum theories and, mainly, Eringen's nonlocal elasticity. They studied research on bending, buckling, and vibration of nanobeams modeled through elementary, Timoshenko, and higher-order nonlocal beam theories. Also, they developed a new hyperbolic shear deformation theory that satisfied traction-free boundary conditions and incorporated transverse shear effects. Qin [25] reviewed recent progress in the study and application of CNTs and graphene-based nanomaterials. Torkaman-Asadi and Kouchakzadeh [26] reviewed the progress in atomistic simulations of graphene's mechanical properties and fracture. Chandel et al. [27] reviewed modeling approaches for nanostructures and explained their mechanical behavior in bending, stability, and vibration. They described processing and fabrication methods and applications in sensors, actuators, composites, and probes. The paper also reported theoretical modeling methods such as atomistic simulations, continuum mechanics, and atomistic–continuum approaches. Roudbari et al. [4] reviewed different size-dependent continuum mechanics models for micro- and nano-structures. Moreover, they focused on applications in bending, buckling, vibration, and wave propagation. The paper explained couple stress, strain gradient models, Eringen's nonlocal elasticity, micromorphic theory, and hybrid nonlocal strain gradient models, and compared their uses and limits. The authors showed that nonlocal elasticity usually predicted softening, while couple stress and strain gradient models predicted hardening at small scales.

A wide variety of analytical and numerical methods have been developed to solve the governing equations of nanomechanics theories. For relatively simple geometries, analytical and semi-analytical techniques, such as separation of variables, Fourier and Laplace transforms, and perturbation expansions, have been used to obtain closed-form or approximate solutions for vibration, buckling, and wave propagation problems [28,29]. Energy-based approaches, including Rayleigh–Ritz [30] and Galerkin methods [31], remain popular for deriving eigenfrequencies and stability criteria in nanobeams and nanoplates. For higher-order continuum theories, such as strain gradient or couple stress elasticity, differential models, including the finite difference method (FDM) [32] and the differential quadrature method (DQM) [33], have been used. The finite element method (FEM) is a general and widely used numerical formulation that can solve many problems in nanomechanics, from simple to highly complex geometries or boundary conditions [34,35]. Isogeometric analysis (IGA), based on smooth spline basis functions, has emerged as an alternative because it naturally provides the continuity required for higher-order gradient models [36,37]. Mesh-free methods, such as the element-free Galerkin (EFG) method and reproducing kernel particle method (RKPM), have also been applied to nanoscale problems, also in large deformation and crack modeling. For fracture behavior, peridynamic discretization methods have gained considerable attention, since they inherently capture discontinuities without additional criteria for crack initiation or growth [38]. At the atomistic scale, MD simulations [39] and density functional theory (DFT) calculations [40] are frequently employed to obtain size-dependent material constants and to validate contin-

uum predictions, while multiscale approaches such as the QC method effectively bridge atomistic and continuum domains [41,42].

Also, recently, there have been many papers published regarding nanomechanics. These investigations have provided deeper insights into the mechanical, electrical, and thermal responses of nanoplate systems, which can be used for the development of advanced nanodevices and multifunctional smart materials [43,44]. For example, Akpınar et al. [45] studied the longitudinal vibration of FG nanotubes in an elastic medium. By applying Bishop's rod theory together with Eringen's nonlocal elasticity, they transformed the boundary condition problem into an eigenvalue formulation using Fourier sine series and Stokes' transformation. Kadioglu and Yayli [46] studied viscoelastic graded nanobeams with elastic spring supports. They found that deformable boundaries reduced the natural frequencies compared to rigid ones, with softer supports leading to greater reductions. They also noticed that damping had a stronger effect on higher vibration modes, though this influence became weaker as the nonlocal scale parameter increased. Yaylı [47] analyzed the buckling of microbeams embedded in an elastic medium. In his study, a Winkler foundation model was used for the surrounding medium, and strain gradient elasticity theory was applied to capture small-scale effects. Yaylı [48] examined the axial vibration of Rayleigh nanorods, which account for rotary inertia effects. Using Eringen's NET, Hamilton's principle, and Fourier–Stokes methods, he derived a general eigenvalue solution that was valid for both rigid and deformable supports. Imani Yengejeh et al. [22] examined the mechanical response of CNTs with atomic and structural imperfections. Using both computational and experimental findings, they concluded that any level of imperfection reduces the mechanical performance of CNTs. Darban [49] studied the size-dependent behavior of silicon nanobeams using large-scale MD simulations. Civalek [50] investigated the free vibration of short fiber-reinforced nano/rods in an elastic medium. Kafkas et al. [51] examined the thermal vibration of perforated nanobeams resting on a Winkler elastic foundation with NSGT.

In recent years, a large number of studies have been published on various aspects of nanomechanics, reflecting the growing importance and rapid progress of this field. These works have provided valuable insights into the mechanical, thermal, and electrical responses of nanoscale systems, as well as their applications in advanced nanodevices and smart materials. However, despite much research, the results are still in different theories and methods. Therefore, there is a clear need for a comprehensive updated review that classifies and discusses the existing nanomechanics theories and numerical methods. The purpose of this paper is to fulfill this need by presenting an updated overview of the current state of research, highlighting the advantages, limitations, and future prospects of various modeling and solution techniques in nanomechanics.

2. Overview of Nanomechanics Theories

The literature mainly focuses on the NET, CST, and NSGT, as these models effectively capture size-dependent mechanical behavior through explicit length-scale parameters while remaining consistent with classical continuum mechanics. They provide a good balance between physical accuracy and computational efficiency, and their predictions agree well with MD results. Moreover, numerous studies have applied these theories to bending, vibration, and buckling analyses, highlighting their broad applicability. Among various nanoscale materials, carbon-based structures such as graphene sheets and carbon nanotubes are of particular interest because of their remarkable mechanical and multifunctional properties [52].

Graphene, a single layer of carbon atoms arranged in a hexagonal lattice, and it can combine in multiple layers to form graphite. When a single graphene sheet is rolled up, it

forms a single-walled carbon nanotube (SWCNT), while rolling up multiple graphene layers produces multi-walled CNTs (MWCNTs) [43]. Figure 1 illustrates the relationship between graphene, graphite, and CNTs. These nanostructures exhibit mechanical behaviors that deviate from classical predictions, so researchers have developed advanced nanomechanics theories to accurately describe their size-dependent responses.

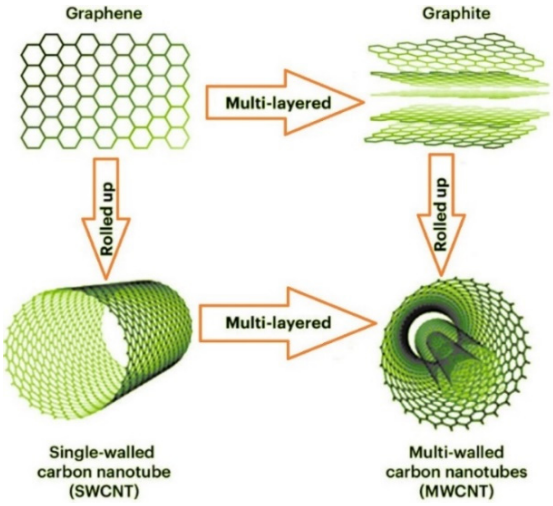

Figure 1. The structural relationship among graphene, graphite, and CNTs [53].

Figure 2 illustrates some of the most common structural forms encountered in nanomechanics. At the nanoscale, materials can be engineered into different geometries such as rods [54–58], beams [59–63], cylindrical shells [64–68], rings [69,70], disks [69,71], and plates [72,73], each offering unique mechanical and physical behaviors. These structures form the basis for studying how size, shape, and dimensional constraints influence mechanical properties such as strength, flexibility, and stability at the nanoscale. Using these geometries, researchers can design nanostructures for applications in sensors, actuators, energy devices, advanced materials, etc.

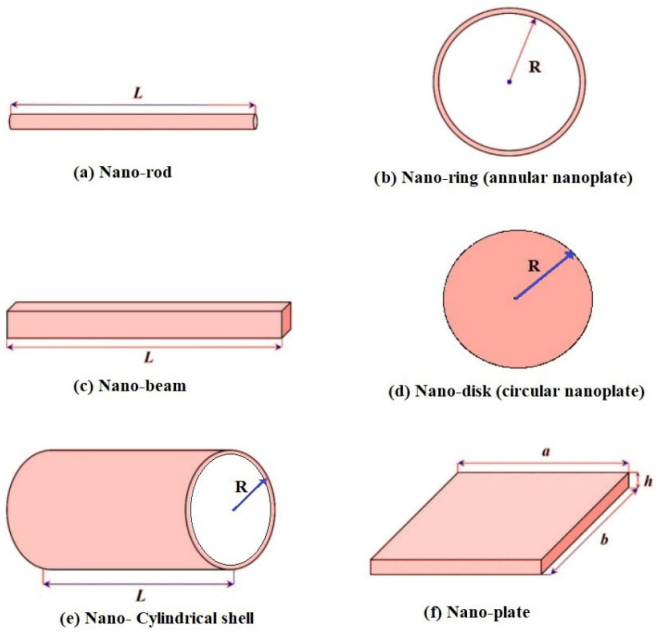

Figure 2. Common structures studied in nanomechanics include the following: (**a**) nanorod, (**b**) nanoring, (**c**) nanobeams, (**d**) nano-disk (circular nanoplate), (**e**) nanocylindrical shell, and (**f**) nanoplates (in this figure R is the radius, L is the length, and a and b are arbitrary dimensions of the plate).

Let x denote the position vector in a body $\Omega \subset R^3$, t time, and $u(x,t)$ as the displacement field. The (small-strain) tensor is $\varepsilon = 12(\nabla u + (\nabla u)^\top)$, and the Cauchy stress is σ. The fourth-order elasticity tensor is C (components C_{ijkl}). The mass density is ρ, body force is b, and ∇ is the spatial gradient, $\nabla \cdot$the divergence, and ∇^2 the Laplacian. Also, a superposed "s" indicates surface quantities defined on a surface S with unit normal n; ∇_s is the surface gradient/divergence and I_s the in-surface identity. The Levi–Civita tensor is ϵ. Intrinsic material lengths are written ℓ, μ, ...

2.1. NET

NET introduces the concept that the stress at a given point depends not only on the strain at that point but also on strains in a finite surrounding region. Eringen's integral form expresses this as [74]:

$$\sigma_{ij}(x) = \int_{\Omega} \alpha(|x - x'|) C_{ijkl} \varepsilon_{kl}(x') dx' \tag{1}$$

where α is a function which describes the nonlocal influence. In a differential approximation, the equation can be written as follow [5]:

$$(1 - \mu \nabla^2)\sigma_{ij} = C_{ijkl}\varepsilon_{kl} \tag{2}$$

where μ introduces an intrinsic length scale. Physically, this accounts for long-range interatomic interactions absent in classical elasticity.

NET has been widely applied to carbon nanotubes, graphene sheets, nanobeams, and nanoplates. There are some of the main limitations and problems associated with Eringen's NET. Firstly, the integral formulation of nonlocal elasticity makes it difficult to define boundary conditions accurately (especially in beam and plate problems such as cantilever bending) [75,76]. For instance, the differential form sometimes fails to satisfy the integral equation at boundaries, making some problems ill-posed [76,77]. Secondly, the integral and differential versions of Eringen's theory can yield contradictory predictions under certain boundary/load settings. For example, some solutions using the differential form show no softening (or even stiffening), contrary to the expected behavior. This discrepancy is sometimes called the nonlocal paradox [14,75]. Thirdly, Eringen's differential nonlocal elasticity may fail to satisfy self-adjointness and conservation properties, which can lead to nonphysical results (for example, an increase in natural frequency with increasing length scale) in certain configurations. Such inconsistencies are caused by the constitutive form not always deriving from a well-defined energy functional [78–80]. Fourthly, purely nonlocal boundary value problems are sometimes ill-posed. It means they may have no unique or stable solution under typical boundary conditions. Some authors argue that for certain beam problems, the only solution in the purely nonlocal theory is trivial or nonexistent [81–83]. Fifthly, the attenuation (kernel) function α (governing how influence decays with distance) is not uniquely defined, and different kernels produce divergent results. Because there is no universal physical basis for the choice of kernel, its selection (and the scaling parameter μ) is often based on experiments or fit to molecular simulations, which limits its general applicability [75]. Sixthly, the integral form involves domain-wide interactions, making it computationally expensive, particularly in 3D or complex geometries. Also, the need to compute double integrals or other complex integral operations can be difficult in large-scale problems [75,84]. Finally, the original linear nonlocal theory is not easily generalized to nonlinear behavior, large deformations, or time-dependent effects without additional assumptions or modifications, which may introduce inconsistencies.

Because interactions are nonlocal, capturing large strain kinematics or dynamic coupling can become quite complex [75,85].

2.2. Strain Gradient Theory

Strain gradient elasticity extends the constitutive law by including not only strains but also their gradients. In Mindlin's and Fleck–Hutchinson's formulations, the stress tensor is written as follows [86]:

$$\sigma_{ij} = C_{ijkl}\varepsilon_{kl} + l^2 D_{ijklmn}\nabla_m \varepsilon_{kl,n} \tag{3}$$

where l is a characteristic material length. This formulation accounts for additional stress terms related to the energy associated with strain gradients. It effectively models the size-dependent behavior observed in experiments, such as increased stiffness and strength in small-scale materials, indentation, and thin films. Strain gradient theory is not itself a nanomechanics theory, but since it accounts for size effects, it is often used as a tool in nano/micro-mechanics [16,87,88].

2.3. CST/MCST

CST introduces additional degrees of freedom associated with material rotation and curvature. In its modified form, the constitutive relations are written as follows [89]:

$$\sigma_{ij} = C_{ijkl}\varepsilon_{kl},\ \mathrm{m}_{ij} = \mu l^2 \chi_{ij} \tag{4}$$

where m_{ij} is the couple stress tensor and χ_{ij} is the symmetric curvature tensor. This theory is able to predict size-dependent effects in bending, torsion, and shear of small-scale structures. Applications range from nanobeams and nanoplate bending to biomechanical tissues such as bone. While conceptually simpler than strain gradient theory, it still introduces additional parameters that require careful experimental calibration.

CST and MCST introduce one or more material length-scale parameters to capture size effects. However, these parameters cannot be directly measured and must often be determined by fitting experimental or atomistic data, leading to inconsistencies and non-unique results across different studies [90,91]. The physical meaning of the additional quantities, such as the couple stress tensor and curvature tensor, is often unclear. Several authors have noted that the symmetric couple stress assumption in MCST lacks solid physical justification and may even contradict fundamental continuum mechanics principles [89,92]. CST requires additional boundary conditions related to moments or rotations. However, the correct mathematical and physical formulation of these boundary conditions remains controversial and difficult to implement, particularly in the modified version [93,94]. Because MCST involves higher-order spatial derivatives of displacement (curvature terms), numerical implementation requires continuous finite elements or special higher-order formulations. This significantly increases computational cost and model complexity compared to classical elasticity [90,91]. Although CST and MCST are designed to capture size effects, they remain continuum-level theories. As the characteristic length approaches atomic dimensions, they fail to represent discrete lattice and molecular behaviors accurately, making atomistic or nonlocal models more suitable in that range [6,95]. The MCST typically assumes isotropy and uses a single scalar length-scale parameter, which simplifies modeling but limits its applicability to anisotropic, layered, or FG materials. So, for these materials, the theory becomes insufficient or less accurate [95,96]. Despite numerous analytical and numerical studies, experimental validation of CST and MCST remains inconsistent. Most available results concern nanobeams or plates under bending, while comprehensive testing for 3D stress states, torsion, and shear is still lacking [91,95].

2.4. NSGT

The NSGT combines features of both nonlocal elasticity and strain gradient formulations. A typical form is as follows [97]:

$$(1 - \mu\nabla^2)\sigma_{ij} = C_{ijkl}(\varepsilon_{kl} + l^2\nabla^2\varepsilon_{kl}) \tag{5}$$

This theory captures both long-range interatomic forces and short-range gradient hardening, which provides a more comprehensive description of nanostructural mechanics. It has been applied to graphene nanoribbons, CNTs, and advanced nanocomposites.

NSGT tries to combine the ideas of nonlocal elasticity and strain gradient theory to describe how materials behave at very small scales. Researchers have found several problems with it. Firstly, NSGT can be mathematically inconsistent when used for structures of limited size. Mixing nonlocal and gradient terms sometimes gives results that do not make physical sense or have no solution. Zaera et al. [98] showed that the theory can fail for finite structures, and Shaat [99] explained that joining nonlocal and strain gradient models can cause contradictions. Another problem is with boundary conditions. Because NSGT has higher-order terms, it needs extra boundary conditions related to the gradients of strain and stress. Many studies use these conditions in an arbitrary way, which can lead to wrong or incomplete results. Barretta et al. [100] pointed out that incorrect boundary conditions can remove the expected nonlocal effects and suggested a consistent way to define them. The theory also shows overlap between nonlocal and gradient effects. Both parts can already explain size-dependent behavior, so combining them may repeat the same physical effect instead of adding new information. Shaat [99] and Aifantis [101] both warned that this overlap can make the theory confusing and less useful. Another difficulty is the large number of parameters in the theory. It needs several length-scale values that are hard to find from experiments. These values are often chosen by fitting data, which makes the results uncertain and not unique [14,98,102]. NSGT is also computationally complex. The equations include higher-order derivatives, which require special numerical methods and more computer time. This makes it harder to use than simple elasticity models [98,101]. Although it is more advanced than classical elasticity, NSGT is still a continuum model. It cannot fully describe what happens at the atomic level, where discrete and quantum effects become important [98,101]. Finally, there is a lack of experimental evidence to confirm NSGT predictions. While it has been applied to nanobeams, graphene sheets, and nanotubes, only a few experiments exist to test it in different conditions. Many reviews mention that more experimental work is needed to verify this theory [14,103].

2.5. Surface Elasticity

At the nanoscale, surface effects play a dominant role. The Gurtin–Murdoch surface elasticity model treats the surface as an independent elastic membrane endowed with its own stress–strain relations. The surface stress tensor is written as follows [104]:

$$\tau^s_{\alpha\beta} = \tau^0_{\alpha\beta} + C^s_{\alpha\beta\gamma\delta}\varepsilon^s_{\gamma\delta} \tag{6}$$

where $\tau^0_{\alpha\beta}$ is the residual surface stress and $C^s_{\alpha\beta\gamma\delta}$ are surface elastic constants. This framework explains the size dependence of stiffness and strength in nanowires, thin films, and core–shell structures where surface-to-volume ratios are large.

2.6. Micropolar (Cosserat) Elasticity

Micropolar or Cosserat elasticity generalizes continuum mechanics, allowing each material point to possess independent translational and rotational degrees of freedom. This

leads to asymmetric stress tensors and couple stresses. The governing balance laws are as follows [105]:

$$\sigma_{ij} + b_i = \rho\ddot{u},\ \mathrm{m}_{ij} + \varepsilon_{ijk}\sigma_{jk} + c_i = J\ddot{\phi}_i \tag{7}$$

where m_{ij} is the couple stress tensor, ϕ_i the microrotation vector, c_i body couples, and J the microinertia. Micropolar models are suited for materials with intrinsic microstructures, such as lattice solids, granular materials, and biological tissues. The limitation lies in the difficulty of experimentally identifying the large number of additional constitutive parameters.

2.7. Peridynamics

Peridynamics differ fundamentally from the PDE-based continuum frameworks and express momentum balance in integral form [106]:

$$\rho(x)\ddot{u}(x,t) = \int_{\Omega} f(u(x',t) - u(x,t), x' - x)dx' + b(x,t) \tag{8}$$

where f is a pairwise force function. Unlike classical continuum mechanics, peridynamics naturally accommodates discontinuities such as cracks without the need for special criteria. It has been used to study fractures in graphene, ceramic nanostructures, and nanocomposites. However, peridynamics are computationally expensive and require calibration of nonlocal kernels.

Comparison of major nanomechanics theories can be seen in Table 1:

Table 1. Comparison of major nanomechanics theories.

Theory	Main Idea	Some Applications	Limitations
NET, Eringen	Stress at a point depends on the strain field of surrounding points.	Vibration [107], buckling [107], and wave propagation [108] in nanobeams, nanoplates, and CNTs.	Only predicts stiffness softening; The nonlocal effect reduces at larger scales.
CST/MCST	Characteristic length introduced through internal moments.	Bending [109], buckling [110], and vibration [111] of nanobeams, nanoplates, and CNTs.	Determining characteristic length experimentally is difficult; limited to simple geometries.
Surface Elasticity (Gurtin–Murdoch Model)	Surface/interface energy incorporated into constitutive relations.	Nanoparticles [112], nanowires [113], thin films [114], graphene sheets [115].	Surface elastic constants must be extracted from MD/DFT or experiments.
NSGT	Combination of NET and SGT to capture both softening and hardening.	More accurate prediction of vibration, buckling [116], bending [71], and wave dispersion [117] in nanostructures.	Higher computational cost; multiple parameters to calibrate.
Peridynamics	Integral-based nonlocal formulation without spatial derivatives.	Fracture [118], crack initiation and propagation [119] in nanostructures.	High computational demand; tricky boundary conditions.

Moreover, Table 2 compares the parameters introduced in each of the main nanomechanics theories, together with their physical interpretation and typical reported ranges in the literature [24,110,120,121].

Table 2. Comparison of key parameters in size-dependent nanomechanics theories.

Theory	Parameters	Physical Meaning	Typical Range
NET [121]	Nonlocal parameter ($\mu = (e_0 a)^2$)	Defines the range of long-range interatomic interactions; e_0 is dimensionless, and a is the internal characteristic length.	$\frac{e_0 a}{L} \approx 0.1 - 2.0$
CST [110]	Length-scale parameter (l_c)	Characterizes rotational gradients and couple-stress effects; relates to internal bending resistance at microscale.	$l_c \approx 1 - 50$nm
NSGT [120]	Nonlocal parameter ($\mu = (e_0 a)^2$) and gradient parameter (ls)	Combines long-range nonlocal softening and short-range strain gradient hardening.	$\frac{e_0 a}{L} \approx 0.1 - 1.0$, $\frac{l_s}{L} \approx 0.05 - 0.5$

3. Numerical and Mathematical Methods

The mechanical behavior of nanostructures governed by nonclassical continuum theories and atomistic models cannot be captured by a single computational approach. A wide range of numerical and mathematical methods has been developed to solve governing equations, from exact analytical formulations to hybrid data-driven strategies. In this section, we review these approaches.

3.1. Analytical and Semi-Analytical Methods

Analytical or semi-analytical techniques are applicable when geometries and boundary conditions are relatively simple. A common strategy is the method of separation of variables, in which the displacement field is assumed in a product form: $u(x,t) = X(x)T(t)$. Substitution into the governing PDEs decouples the spatial and temporal parts, producing ordinary differential equations that can be solved separately. Resulting spatial eigenfunctions $X(x)$ and temporal functions $T(t)$ are then combined to form modal solutions. Integral transform methods, such as the Fourier and Laplace transforms, are also widely used. For instance, applying a Fourier transform in space and time leads to a representation, as follows [122]:

$$\hat{u}(k,\omega) = \int_{-\infty}^{\infty} \int_{0}^{\infty} u(x,t) e^{-i(kx-\omega t)} dx dt \tag{9}$$

where k is the wave number and ω the angular frequency. This converts differential operators into algebraic multipliers, simplifying the analysis of wave dispersion in nonlocal models. When exact solutions are not feasible, approximate variational techniques are employed. In the Ritz method, the displacement field is approximated as follows [123]:

$$u(x) \approx \sum_{i=1}^{N} a_i \phi_i(x) \tag{10}$$

with admissible shape functions ϕ_i and unknown coefficients a_i. These coefficients are determined by minimizing the total potential energy. Similarly, the Galerkin method enforces the residual of the governing PDE to be orthogonal to all chosen test functions, producing a set of algebraic equations.

3.2. Differential Methods

Over the past decades, numerical techniques in nanomechanics have evolved significantly in terms of accuracy, computational efficiency, and applicability to complex boundary conditions. Early analyses often relied on the FDM due to its conceptual simplicity and ease of implementation; however, its low-order accuracy and mesh dependency limited its effectiveness for nanoscale systems [124].

Differential discretization schemes directly approximate derivatives in the governing PDEs. The FDM replaces derivatives with discrete difference quotients. For example, the second derivative at node x_i is approximated as follows [124]:

$$\left.\frac{d^2u}{dx^2}\right|_{x_i} \approx \frac{u_{i+1} - 2u_i + u_{i-1}}{\Delta x^2} \tag{11}$$

where Δx is the grid spacing and $u_i = u(x_i)$. Once all derivatives are replaced, the PDE reduces to a system of linear or nonlinear algebraic equations, which can be solved by direct or iterative solvers.

To overcome FDM shortcomings, the DQM was introduced, offering higher-order precision by approximating derivatives using weighted sums over all grid points [125]. The DQM provides a more accurate approximation by expressing derivatives as weighted sums of function values at all grid points [126]:

$$\left.\frac{du}{dx}\right|_{x_i} \approx \sum_{j=1}^{N} \omega_{ij} u(x_i) \tag{12}$$

with ω_{ij} denoting weighting coefficients derived from interpolation functions. The resulting algebraic system is typically dense but offers high accuracy with fewer nodes.

More recently, spectral methods [127] have gained attention for their superior convergence rates and ability to achieve near-exact solutions with relatively few nodes, especially when dealing with nonlocal elasticity or gradient theories. Spectral methods instead expand the solution into orthogonal basis functions, such as Chebyshev polynomials or Fourier series. The expansion coefficients are obtained by enforcing the PDE in weak or collocation form.

For boundary value problems, the shooting method is often applied. The original problem is converted into an initial value problem by guessing unknown initial conditions, integrating the ODE system (commonly with Runge–Kutta), and iteratively adjusting the guesses until boundary conditions are satisfied [128].

For clarity, Table 3 compares the key characteristics of the differential methods discussed above, highlighting their relative advantages, disadvantages, and common applications in nanomechanics.

Table 3. Comparison of differential numerical methods in nanomechanics.

Method	Main Principle	Advantages	Disadvantages	Typical Applications
FDM	Approximates derivatives by finite differences on a discrete grid.	Simple to implement; suitable for regular geometries; easy to program; low memory demand.	Accuracy depends on mesh density; less effective for complex geometries or irregular boundaries; difficulties with higher-order derivatives.	Bending [129], buckling [130], and vibration [131] of usually simple geometries such as beams and plates.
DQM	Approximates derivatives using weighted sums of function values at all grid points.	Very high accuracy with few grid points; efficient for higher-order PDEs; good convergence.	Produces dense coefficient matrices; less efficient for large or irregular domains; boundary treatment can be complex.	Bending [132], buckling [133], vibration [134] of beams, plates, shells, or complex structures [135].
Spectral Methods	Expands the solution in orthogonal basis functions (e.g., Chebyshev or Fourier series).	Spectrally high accuracy ("exponential convergence"); excellent for smooth solutions; handles periodic domains naturally.	Requires smooth geometry; less effective for discontinuities or complex boundaries; implementation is more mathematical.	Wave propagation [136], vibration [137], and stability of nanostructures with regular boundaries [138].

3.3. Energy-Based Approaches

Energy-based formulations are rooted in variational principles. According to Hamilton's principle, we have the following [139]:

$$\delta \int_{t_1}^{t_2} (T - U + W) dt = 0 \tag{13}$$

where T is the kinetic energy, U is the strain energy, and W is the work of external forces. For example, the strain energy of a nanobeam in nonlocal elasticity can be expressed as follows [139]:

$$U = \frac{1}{2} \int_0^L EI(\frac{\partial^2 \omega}{\partial x^2}) dx \tag{14}$$

with E as the Young's modulus, I as the second moment of area, and $\omega(x,t)$ as the transverse displacement. The displacement field is approximated by a finite series expansion. Substitution into the functional yields an expression in terms of unknown coefficients. Minimizing the functional with respect to these coefficients generates algebraic equations, which can be solved to obtain equilibrium or vibration characteristics.

3.4. Finite Element Extensions

The FEM has been extensively extended to accommodate higher-order continuum models. In gradient elasticity, where governing equations contain second gradients of displacement, shape functions must ensure continuity (continuity of displacement and slope). Hermite polynomials are commonly used for this purpose. IGA addresses geometry and approximation simultaneously. Here, the displacement is approximated with non-uniform rational B-splines (NURBS) [140]:

$$u(\xi) = \sum_{i=1}^{n} R_i(\xi) d_i \tag{15}$$

where $R_i(\xi)$ are NURBS basis functions and d_i are the unknown control point variables. This direct link with CAD geometry enhances accuracy and smoothness.

Mesh-free methods, such as the element-free Galerkin (EFG), the reproducing kernel particle method (RKPM), and smoothed particle hydrodynamics (SPH), do not require a predefined mesh. The displacement field is approximated as follows [141]:

$$u(x) \approx \sum_{i=1}^{N} \phi_i(x) u_i \tag{16}$$

where ϕ_i are kernel-based shape functions and u_i are nodal parameters. These methods are particularly well-suited for problems involving cracks and large deformations, as they naturally handle discontinuities.

3.5. Integral Formulations

Nonlocal and fracture-dominated problems are efficiently handled by integral formulations. In peridynamics, the classical PDE is replaced by an integral equation [142]:

$$\rho(x)\ddot{u}(x,t) = \int_{H_x} f(u(x',t) - u(x,t), x' - x) dV_{x'} + b(x,t) \tag{17}$$

where $\rho(x)$ is the density, $u(x,t)$ the displacement, H_x is the horizon (a finite neighborhood around point x), f is the pairwise force function, and $b(x,t)$ is the body force. This formulation avoids singularities and naturally captures crack initiation and growth by bond breakage. The boundary element method (BEM) reduces PDEs to boundary integral equations using fundamental solutions, requiring discretization only of the boundary. This reduces problem dimensionality but requires the availability of Green's functions.

3.6. Atomistic and Multiscale Methods

Atomistic simulations capture nanoscale physics directly. In MD, the motion of each atom is governed by Newton's second law [143]:

$$m_i \ddot{r}_i = -\nabla_i U(r_1, r_2, \ldots r_N) \tag{18}$$

where m_i is the mass of atom i, $\ddot{r}_i$ its position, and U is the interatomic potential energy.

DFT focuses on electronic structure, solving the Kohn–Sham equations [143]:

$$\left[\frac{h'^2}{2m_e}\nabla^2 + V_{eff}(r)\right]\psi_i(r) = \in_i \psi_i(r) \tag{19}$$

where h' is the reduced Planck constant, m_e is the electron mass, V_{eff} is the effective potential, ψ_i is the electron wavefunction, and $\in_i$ is its eigenenergy. The solution is obtained self-consistently until the total energy converges.

3.7. Semi-Analytical Special Techniques

Several perturbative and decomposition methods are designed to handle nonlinear governing equations. The Adomian decomposition method (ADM) expresses the solution as an infinite series, $u(x) = \sum_{m=0}^{\infty} u_n(x)$, and expands nonlinear operators into Adomian polynomials. Each part is found by repeating the same rule, and this makes it reach the final result faster when the system is not nonlinear [144].

In the numerical modeling of nanoscale structures, the convergence of the applied methods was examined through mesh or grid refinement studies. For example, in the FDM, convergence is verified by reducing the grid size (Δx) until successive solutions show negligible variation. Mohamed et al. [145] examined the convergence of a sixth-order compact FDM for the vibration analysis of Euler–Bernoulli nanobeams. Their results showed that the method achieves rapid convergence for all boundary conditions, providing accurate results even with few grid points. This superior performance arises from the high-order discretization of derivatives and the use of sixth-order boundary treatments, which significantly reduce truncation errors. The inclusion of additional correction terms from Taylor expansions eliminates lower-order errors, allowing the method to reach nearly fourth-order convergence with fewer computational points compared to earlier non-compact schemes [146]. In the DQM, convergence is assessed by increasing the number of grid points (N); as N increases, the computed deflection or frequency values approach a constant limit, typically achieving stable results. For example, Karami et al. [147] investigated the free vibration behavior of triclinic nanobeams using the DQM. The study examined convergence by increasing the number of grid points and showed that the method provides fast and stable convergence, reaching accurate results with as few as 19 nodes. This rapid convergence is attributed to the use of Chebyshev–Gauss–Lobatto sampling points and high-order weighting coefficients, which minimize interpolation and truncation errors. For the FEM, the solution is refined by decreasing the element size or increasing the polynomial order of the shape functions. In the Ritz method, convergence is achieved by successively increasing the number of admissible trial (basis) functions in the assumed displacement

field until key response quantities, such as total potential energy, deflection, or natural frequency, stabilize within a desired tolerance. The rate of convergence can also depend on the applied boundary conditions; for example, the clamped–free boundary condition converges faster with $N = 5$, whereas other cases, such as pinned–pinned, clamped–pinned, and clamped–clamped require around $N = 7$ to achieve the desired accuracy [148]. These convergence studies confirm that the discussed numerical methods can provide accurate and stable results even when nonlocal or gradient-dependent terms dominate in nanoscale continuum models.

4. Applications of Nanostructures

MEMS/NEMS are systems where mechanical motion is combined with electrical circuits. Their sizes are usually on the micro- or nano-scale. Adding nanomaterials to these systems has greatly improved their performance and expanded their range of applications. For instance, CNTs and graphene membranes have been used in resonators, pressure sensors, and microphones, where their low mass and high stiffness enable resonance frequencies in the megahertz to gigahertz range and provide high sensitivity. Nanowires and nanoparticles are also incorporated into MEMS/NEMS to increase sensing performance, especially in gas and biosensors, where high surface-to-volume ratios maximize interaction with analytes. In addition, nanomaterials have been employed in NEMS actuators and switches, where they offer improved response speeds, lower energy consumption, and multifunctionality, such as simultaneous sensing and actuation [149–151].

5. Case Studies of Nanostructure Analyses

Nanomechanics, as an extension of classical solid mechanics into the nanoscale domain, addresses size-dependent deformation, stability, dynamics, and failure of nanostructures. The following parts summarize the main categories of solid mechanics problems that have been extensively studied for nanoscale systems such as CNTs, graphene sheets, nanobeams, nanorods, nanoplates, and nanoshells.

5.1. Static Analyses in Nanomechanics

Nanostructures are frequently subjected to static loading in bending, axial tension/compression, or torsion. Continuum theories such as nonlocal elasticity, strain gradient theory, couple-stress formulations, and surface elasticity have been applied to study nanostructures. For example, Ke et al. [152] studied the static and dynamic responses of doubly curved FG porous nanoshells with piezoelectric surface layers with FEM while considering the flexoelectric effect and using refined higher-order shear deformation theory (HSDT) as well as NET. Their results showed that flexoelectricity and nanoscale size effects strongly influenced bending, vibration, and transient responses. Additionally, factors such as porosity distribution, curvature radius, and foundation stiffness significantly affected the electromechanical behavior, providing insights for designing nanoscale devices such as sensors and semiconductor components. Omar et al. [153] investigated the static stability of FG porous nanoplates subjected to uniform and nonuniform in-plane loads using the NSGT and Galerkin method. Their findings revealed that nonlocal and strain gradient parameters, porosity distribution, and loading type significantly affected critical buckling load. Uniform porosity tended to reduce stiffness, while non-uniform porosity distributions improved stability. Also, they concluded that increasing foundation stiffness and length-scale parameters enhanced the buckling resistance of the nanoplates.

Brischetto and Cesare [154] developed an exact three-dimensional shell model for the static and free vibration analysis of multilayered magneto-elastic structures containing piezomagnetic materials. They formulated four coupled second-order differential equa-

tions linking displacements and magnetic potential within a mixed curvilinear orthogonal system. The solution was obtained using harmonic functions in-plane and the exponential matrix method through thickness. Their results showed that magneto-elastic coupling, material layer arrangement, and thickness effects significantly influenced static deformations and natural frequencies, offering accurate predictions for the design of multilayered smart actuators and sensors. Anh et al. [155] analyzed the nonlinear static behavior of magneto-electro-elastic sandwich micro/nano-plates with a FG carbon nanotube core in a hygrothermal environment using Eringen's nonlocal elasticity and the Galerkin method. Also, parametric studies investigated CNT reinforcement patterns, nonlocal parameters, thermal and moisture variations, and electric/magnetic potentials. The results demonstrated that increasing CNT volume fraction and nonlocal parameters enhanced stiffness, while hygrothermal loads reduced structural resistance. The study highlighted the efficiency of FG-CNT cores in improving the mechanical and multifunctional performance of magneto-electro-elastic sandwich structures. Genel et al. [156] studied the in-plane static behavior of curved nanobeams using the finite element formulation. They introduced a novel two-noded curved finite element developed from exact analytical solutions of governing equations using NET. Their findings showed that the proposed method provided highly accurate results with reduced computational cost, making it an efficient approach for investigating the in-plane static response of curved nanobeams at the nanoscale.

Siddique and Nazmul [109] studied the static bending behavior of bidirectional FG nanobeams using the nonlocal CST and NSGT. They derived closed-form analytical solutions by applying Hamilton's principle and the Laplace transform technique to capture size effects in nanoscale structures. Also, their results showed that both nonlocal CST and NSGT successfully described size-dependent behaviors, but NSGT generally predicted larger displacements, and, consequently, overestimated size effects compared to NCST (as can be seen in Table 4). Table 4 shows the comparison of nondimensional maximum displacement values of nanobeams analyzed using NSGT and nonlocal couple stress theory (NCST). The parameters include the nonlocal parameter (μ), boundary condition, and material gradation parameter (β). In the Table, l_s is the strain gradient length scale (for NSGT) representing strain gradient effects, while l_c is the couple stress length scale (for NCST) representing microrotation effects in nanostructures. The values are nondimensional displacements. NSGT tends to predict slightly higher deflections, indicating stronger size-dependent effects. It is noted that, in Table 4, the reduction in displacement with increasing material gradation parameter β in both NSGT and NCST models is mainly attributed to the enhancement of the effective stiffness of the beam along its length. As β increases, a larger portion of the beam is composed of the stiffer constituent material, resulting in an increase in the effective bending rigidity and, consequently, a decrease in the overall deflection.

Wu et al. [157] studied the nonlinear static behaviors of nonlocal nanobeams subjected to a longitudinal linear temperature gradient based on the nonlocal stress gradient theory and using the Galerkin method. They noticed that the nonlocal effect was found to play a major role in altering deformation amplitudes and stability. Rasouli et al. [158] examined the dynamic buckling of FG graphene platelet-reinforced composite beams under axial harmonic loading using NSGT. Employing Reddy's shear deformation theory and the DQM, they showed that increasing graphene platelet content and adopting an X-type distribution enhanced buckling resistance. In contrast, larger nonlocal parameters reduced stability, while greater strain gradient length scales and clamped boundaries improved it. Zheng et al. [159] studied the size-dependent nonlinear bending behavior of magneto-electro-elastic laminated nanobeams resting on an elastic foundation using Reddy third-order shear deformation theory combined with nonlocal elasticity and von Kármán geometric nonlinearity and the Galerkin method. Their results showed that

the nonlocal parameter reduced flexural stiffness, reflecting the softening effect at the nanoscale. Increasing Winkler and Pasternak foundation parameters enhanced stiffness. Also, Soltani et al. [160] studied the stability of sandwich double-nanobeam systems with varying cross-sections interconnected by a Kerr-type three-parameter elastic layer. They modeled two parallel tapered sandwich nanobeams joined through an elastic Kerr foundation, with material properties varying exponentially along the length using Eringen's NET, the Euler–Bernoulli beam model, and the generalized DQM. Their results showed that parameters such as the tapering ratio, nonlocal parameter, thickness ratio, volume fraction index, axial load ratio, and stiffness of the elastic connections had significant influence on the critical buckling load. Ren et al. [161] studied the bending and buckling of FG piezoelectric Timoshenko nanobeams using a two-phase local/nonlocal piezoelectric integral model using the generalized DQM. They showed that increasing the nonlocal length parameter raised deflections and lowered buckling loads, whereas increasing the local volume fraction achieved the opposite.

Table 4. Comparison of nondimensional maximum displacement of nanobeam in clamped (C) and simply supported (S) boundary conditions [109].

μ	Boundary	β	NSGT (ls = 1.0)	NSGT (ls = 0.5)	NSGT (ls = 0)	NCST (lc = 1.0)	NCST (lc = 0.5)	NCST (lc = 0)
0	S-S	0.5	0.00130	0.00135	0.00138	0.00025	0.00064	0.00138
		1.0	0.00102	0.00107	0.00109	0.00019	0.00050	0.00109
		1.5	0.00081	0.00085	0.00086	0.00015	0.00040	0.00086
	C-C	0.5	0.00019	0.00025	0.00027	0.00005	0.00013	0.00027
		1.0	0.00015	0.00019	0.00021	0.00004	0.00010	0.00021
		1.5	0.00012	0.00015	0.00016	0.00003	0.00008	0.00016
1	S-S	0.5	0.00143	0.00149	0.00151	0.00027	0.00070	0.00151
		1.0	0.00113	0.00117	0.00119	0.00021	0.00055	0.00119
		1.5	0.00090	0.00093	0.00095	0.00017	0.00044	0.00095
	C-C	0.5	0.00019	0.00025	0.00027	0.00005	0.00013	0.00027
		1.0	0.00015	0.00019	0.00021	0.00004	0.00010	0.00021
		1.5	0.00012	0.00015	0.00016	0.00003	0.00008	0.00016

Some static analyses related to nanomechanics are summarized in Table 5.

Table 5. Summary of recent static analyses in nanomechanics.

Ref.	Type of Analysis	Type of Theory	Numerical/Analytical Method	Key Findings
[162]	Static torsional analysis of FG nanobeams	Stress-driven nonlocal integral elasticity	analytical–semi-analytical	New nonlocal foundation model overcomes Eringen–Wieghardt inconsistencies; accurately captures size-dependent torsional behavior; torsional rotation increases with foundation nonlocal parameter (softening effect); simplified equivalent formulation reduces computational cost
[163]	Static bending of FG nanobeam under electromechanical loading	NSGT	Analytical Navier solution	Static response strongly influenced by applied voltage, power-law index, and scale parameters; positive voltage increases deflection.
[156]	In-plane static bending of curved nanobeams	NET (Eringen's differential form)	Exact-solution-based curved finite element formulation with circular elements	Proposed FE formulation inherits analytical accuracy of nonlocal theory; provides high accuracy at low computational cost.
[164]	Static bending of Euler–Bernoulli and Timoshenko beams	Eringen's nonlocal integral elasticity model	Analytical closed-form solution	First exact closed-form solution of Eringen's nonlocal integral beam model; integral form predicts consistent softening with nonlocality.
[165]	Static bending, buckling, wave propagation, and vibration of hollow-core beams	Higher-order beam theory	Exact analytical solutions; FEM	HOE of axial force influences deflection, buckling, frequencies, and wave dispersion; tensile axial force raises, compressive lowers natural frequencies

Table 5. *Cont.*

Ref.	Type of Analysis	Type of Theory	Numerical/Analytical Method	Key Findings
[166]	Static bending and free vibration of FG nanobeams under temperature fields	Nonlocal elasticity and cubic shear strain theory	Closed-form solutions via direct integration and Navier series	Temperature rise increases deflection, lowers frequencies; nonlocality softens response; FG distribution changes stiffness significantly
[167]	Static bending of copper–graphene nanocomposite plate under thermal and mechanical loads	Refined shear-deformable plate kinematics; micromechanical modeling	Analytical via virtual work principle; material properties from experimental/statistical models	Displacements rise with higher thermal loads and folding parameters; decreasing graphene volume fraction lowers stiffness.
[168]	Static bending, free vibration, dynamic response	Nonlocal elasticity + modified couple stress + surface elasticity	IGA with NURBS	Porosity reduces stiffness; surface effects enhance it; IGA accurately captures static and dynamic behavior
[169]	Static bending, thermal buckling, free and forced vibration	Plate theory + nonlocal elasticity; viscoelastic/multiphysics coupling	Analytical Navier-type solution	Thermal loads reduce stiffness and buckling loads; viscoelastic foundation increases damping and modifies vibration; multiphysics strongly influences nanoplate behavior
[170]	Nonlinear static bending of annular nanoplates	Stress-driven theory (SDT) with nonlinear plate formulation	FDM, DQM, Newton–Raphson iteration	Nonlocal stiffening observed; larger scale parameter increases rigidity; SDT provides stable and well-posed formulation for annular nanoplates
[171]	Static bending and free vibration of FG annular nanoplates	Stress-driven theory (SDT) + FGM power-law distribution	Analytical solutions with special functions; Galerkin FEM validation	Increasing nonlocal parameter reduces static deflection and raises natural frequencies; SDT avoids paradoxes of differential nonlocal theory
[172]	Static bending of organic nanoplates in thermal environment	Novel shear deformation plate theory and NET	Closed-form analytical solution with single governing displacement variable	Bending response strongly affected by temperature; reduced-order model with high efficiency; accurate predictions compared with FEM
[173]	Mechanical behavior of nanocircular plates under surface and nonlocal effects	NET + Surface elasticity theory (Gurtin–Murdoch model)	MD simulations and analytical plate model	Surface effects and nonlocal effects strongly affect bending and deflection. Tensile surface stress increases deflection, compressive stress reduces it, and nonlocality decreases deflection. Effects are stronger for smaller thickness.

The authors of Ref. [174] investigated the static bending behavior of laminated composite shells using a nonlocal PD-HSDT approach that combined HSDT with the peridynamic differential operator (PDDO). HSDT captures shear and stress variations, while PDDO introduces nonlocal effects to improve accuracy in complex geometries. The main advantage of PDDO is the ability to express derivatives of any order in an integral nonlocal form without mesh dependency, offering higher precision in stress and deformation analysis. Figure 3 illustrates the computational flow of the proposed method, from defining geometry and material data to applying PDDO, solving the nonlocal equilibrium equations, and evaluating deflections and stresses.

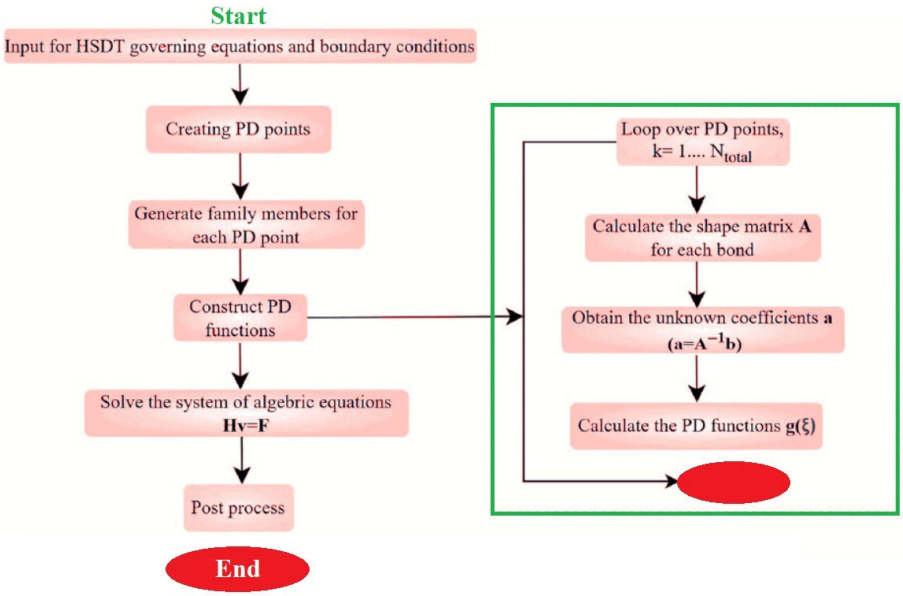

Figure 3. Computational procedure of the PDDO-based HSDT approach [174].

Bab et al. [174] investigated the nonlocal static response of laminated composite shells by embedding a peridynamic differential operator into an HSDT. Table 6 reports the non-dimensional center deflection of cross-ply spherical shells under sinusoidal transverse loading for R/a = 5, 10 and 20, and 3 laminate models (0°/90°, 0°/90°/0°, 0°/90°/90°/0°). The proposed PD-HSDT predictions closely match the exact HSDT solutions of Reddy and Liu across all cases, with relative errors generally below 1% and reaching 0.05% for the 0°/90°/90°/0° laminate, whereas first order deformation theory (FSDT) exhibits noticeably larger discrepancies (approximately 1.7–7.3% depending on laminate and R/a). These comparisons demonstrate that integrating the peridynamic differential operator within HSDT delivers more converged and accurate responses than FSDT for the examined shell configurations [174].

Table 6. Non-dimensional cross-ply spherical shell center deflection (sinusoidal loading). Deflection for three laminations (0°/90°, 0°/90°/0°, 0°/90°/90°/0°) [174].

Theory	R/a	0°/90°	0°/90°/0°	0°/90°/90°/0°
PD-HSDT [174]	5	11.0779	6.7510	6.7834
FSDT [175]	5	11.429	6.4253	6.3623
HSDT [175]	5	11.166	6.7688	6.7865
PD-HSDT [174]	10	11.7985	7.0136	7.0508
FSDT [175]	10	12.123	6.6247	6.5595
HSDT [175]	10	11.896	7.0325	7.0536
PD-HSDT [174]	20	11.9887	7.0825	7.1209
FSDT [175]	20	12.309	6.6756	6.6099
HSDT [175]	20	12.094	7.1016	7.1237

5.2. Buckling Analyses in Nanomechanics

The stability of nanostructures under compressive or axial loading has been widely investigated through buckling and post-buckling analyses. Representative systems include CNTs, nanobeams, nanowires, and nanoshells. Nonlocal beam and shell theories, hygro-thermal coupling models, and surface elasticity effects are employed to capture size-dependent stability behavior. Nonlinear FEMs, such as arc-length continuation and Riks techniques, in combination with MD simulations, provide detailed insight into post-buckling responses. Results consistently show that critical buckling loads are reduced due to nonlocal softening, while post-buckling paths are strongly dependent on geometry and nanoscale parameters. These findings are important for the safe design of CNT-based supports and stable nanoscale devices. Guo et al. [176] studied the nonlinear bending and thermal post-buckling of magneto-electro-elastic nanobeams with nonlocal strain gradient and surface effects. They applied an asymptotic expansion method to solve the nonlinear partial differential equations in closed form. The results showed that nonlocality reduced stiffness, while the strain gradient increased it. Surface elasticity had a role similar to applied electric or magnetic fields. Foundation stiffness raised the critical buckling load, and surface molecules influenced bending more than post-buckling. Lieu et al. [177] investigated thermal buckling of organic solar nanobeams resting on a viscoelastic foundation with NET and HSDT with an analytical solution. The results showed that the critical thermal load had both real and imaginary parts, where the real part caused instability and the imaginary part represented dissipation from the viscoelastic foundation. They found that stronger foundation stiffness delayed buckling, large deformations influenced predictions, and size effects reduced the critical loads compared to classical theory. Sah-

mani et al. [178] analyzed nonlinear asymmetric thermomechanical buckling of shallow nanoscale arches reinforced with FG graphene nanofillers. They used NSGT and extended IGA to capture size effects. The results showed that nonlocality caused softening while strain gradients induced stiffening, and competition between them depended on load and temperature. Zhang et al. [179] examined buckling of graphene nanosheets under local indentation. They combined MD simulations with analytical energy methods to obtain the critical indentation depth. They reported that increasing thickness or changing lattice geometry raised the critical indentation depth, while bonding configurations affected buckling shape and behavior. Hou et al. [180] studied the buckling of CNTs exposed to non-uniform time-dependent heat flux using non-equilibrium MD simulations. The results showed that kinetic energy increased until buckling, then stabilized, and potential energy peaked before dropping negative, and higher heat flux led to stronger local deformation but stabilized the post-buckled state. They also observed that higher flux reduced overall center displacement, indicating localized buckling. Yang et al. [181] investigated post-buckling of porous magneto-electro-elastic nanoplates under mechanical, electric, and magnetic fields. They used NSGT combined with Mindlin plate assumptions and solved the system with the Galerkin method. The results showed that symmetric porosity improved buckling resistance by about 30% compared to asymmetric porosity. They also found that nonlocal effects reduced stability, while strain gradients enhanced it. Sahmani et al. [182] developed a model for thermal buckling of FG porous nano-arches with surface elasticity and nonlocality. They combined Gurtin–Murdoch surface elasticity with nonlocal continuum theory and solved the system using IGA. Their results showed that thin arches were more sensitive to surface effects, while thicker arches displayed stronger nonlocal softening. They also found that porosity distribution influenced stability, with uniform porosity giving more stable responses, and temperature rise increased load magnitudes without changing equilibrium limit points. Ataccan [183] analyzed snap-through buckling of FG sinusoidal shallow nano-arches supported by elastic springs. They applied stress-driven NET with von Kármán strain relations and solved the nonlinear equations using the generalized DQM and Newton–Raphson scheme. Their results showed that snap-through loads were highly sensitive to nonlocal parameters, and supported stiffness and gradation. Stiffer springs raised loads, while stronger nonlocal effects lowered them, and higher modular ratios increased structural stability. Lieu et al. [184] investigated static bending and buckling of FG sandwich nanobeams with auxetic honeycomb cores. They applied third-order shear deformation theory (TSDT) and developed an analytical solution for the governing equations. The results showed that the wall angle of the honeycomb strongly affected mechanical behavior. The study also reported that boundary conditions, material gradation, and geometrical parameters significantly influenced both critical buckling loads and maximum deflections. Tang et al. [185] analyzed buckling/vibration of axially FG nanobeams. They developed a finite element formulation based on Hamilton's principle and incorporated stress- and strain-driven two-phase local/nonlocal integral models. Solutions were obtained with FEM combined with the Lagrangian multiplier method and validated with the generalized DQM. Their results showed that gradient index had more effect on mode shapes than on buckling loads or frequencies, and that nonlocal parameters and boundary conditions strongly influenced critical values. Georgantzinos et al. [186] studied laminated composites reinforced with multi-walled CNTs under combined mechanical, thermal, and moisture effects. They used a multiscale method combining Halpin–Tsai equations, Chamis micromechanical formulas, and finite element analysis. Results showed that increasing CNT content improved buckling resistance. They found that moisture and temperature lowered critical loads, and their predictions matched well with experimental data. Hafed [187] studied tapered FG nanobeams on elastic foundations under compressive loads. She in-

troduced new nonlinear curvature models and combined them with NET. The nonlinear governing equations were solved using fourth- and fifth-order FDMs. Their results showed that nonlinear curvature models reduced critical loads compared to linear ones, variable modulus and inertia strongly influenced buckling resistance, and clamped supports produced the highest critical loads. Sahmani et al. [188] analyzed the nonlinear buckling of FG porous reinforced curved nanobeams with different curvatures. They applied NSGT with two length-scale parameters and solved them using isogeometric collocation. Their results showed that graphene platelet content had a negligible effect on size-dependent influences, especially for high curvatures. For small curvature, reducing porosity increased the role of nonlocal and gradient effects on maximum deflections. For a larger curvature, these effects decreased at the upper limit point but grew at the lower one. Nazmul et al. [62] presented an analytical buckling study of bidirectional FG nanobeams. They used Eringen's NET with Euler–Bernoulli assumptions, derived governing equations by Hamilton's principle, and solved analytically using the Mellin transform. Their findings showed that changing thickness parameters consistently stiffened buckling resistance, with an optimum near unity, while axial gradation also increased stiffness at rates depending on the support condition and buckling mode. Hieu et al. [189] studied the size-dependent buckling of FG carbon nanotube-reinforced composite nanoplates. Also, plates were reinforced with single-walled CNTs embedded in a polymer matrix and arranged in four different reinforcement distributions. The analysis was carried out using a model that combined HSDT with NSGT. Analytical solutions for the critical buckling loads were derived for three types of boundary conditions. The results were verified by comparing them with existing numerical results. The findings showed that increasing the volume fraction of nanotubes enhanced buckling resistance, while higher aspect ratios reduced it. Both the nonlocal parameter and the material length-scale parameter significantly affected the critical loads, demonstrating the need to account for nanoscale size effects in design. Bugday et al. [190] examined the buckling of sandwich nanoplates with auxetic honeycomb cores under combined magnetic and thermal loading using HSDT with thickness-stretching and NSGT. The governing relations were derived through Hamilton's principle and solved by the Navier approach for simply supported conditions. The study showed that the honeycomb architecture and core geometry strongly improved resistance to buckling, while thermal gradients and magnetic fields modified the critical loads.

A summary of buckling/post-buckling studies in nanomechanics can be seen in Table 7.

In nanomechanics, many papers use advanced theories such as nonlocal elasticity, strain gradient, and CSTs to study the buckling and post-buckling behavior of nanoscale structures like nanobeams, nanoplates, and nanotubes. These studies mainly focus on how size effects, geometry, and material variations change the stability and deformation of small-scale structures compared with classical elasticity.

Most studies first examine the critical buckling load and buckling mode shapes. For example, the authors of ref. [205] axially analyzed FG nanobeams using the NSGT. They reported that when the nonlocal parameter increased, the critical buckling load dropped. In contrast, when the strain gradient parameter increased, the critical load increased. This example clearly shows how both small-scale parameters can strongly affect stability. Post-buckling analysis is another common topic. Authors of ref. [206] studied post-buckling of FG nanobeams using the NSGT. They found that for a nanobeam, the nonlocal parameter reduced the post-buckling load, while including strain gradient effects increased it. Their results also showed that the post-buckling deflection was smaller for larger strain gradient parameters, indicating that gradient effects delay large deformation after buckling. Geometry also has a strong influence. Authors of ref. [207] analyzed tapered nanobeams with varying cross-sections under axial compression. For a certain taper ratio, the critical

buckling load decreased. They also showed that this reduction became more significant as the nonlocal parameter increased. Zhang et al. [208] investigated nonlinear post-buckling of nanobeams with nonlocal and gradient effects.

Table 7. Summary of buckling and post-buckling studies in nanomechanics.

Ref.	Type of Analysis	Type of Theory	Numerical/Analytical Method	Key Findings
[191]	Buckling and post-buckling of nano-laminates	Surface elasticity theory with Kirchhoff and Mindlin plate theories	Analytical solutions and Galerkin method	Surface/interface energy strongly affects stability. Positive surface elasticity increases critical load, negative decreases. Residual stress improves stability. Shear deformation reduces stability.
[192]	Thermal buckling of FG nano-sandwich plates with auxetic butterfly cores	HSDT and NSGT	Hamilton's principle and Von Kármán relations, and Halpin–Tsai micromechanics	Graphene reinforcement, FG index, and foam structure improve resistance. Nonlocal effects add flexibility. Useful for aerospace and thermal shielding designs.
[193]	Buckling of FG Bernoulli-Euler nanobeams	Surface stress-driven nonlocal elasticity model and surface elasticity theory	Virtual work principle; parametric numeric study	Coupled surface stress and nonlocal effects significantly influence critical buckling loads. Surface residual stress and stiffness alter stability. Cross-sectional shape and FG index strongly affect buckling.
[194]	Buckling of laminated cylindrical shells in elastic and thermal environments	Extended FSDT and Classical Theory	Extended rule of mixture and MD, and analytical derivations	Elastic foundation and thermal environment influence axial buckling load. CNT distribution patterns and r/h ratio strongly affect resistance. FSDT is more accurate than Classical Theory.
[195]	Buckling of layered cylindrical nanoshells	Refined Zigzag Theory and NSGT and Gurtin–Murdoch surface/interface elasticity	analytical formulation	Interfacial and scale effects significantly influence buckling.
[196]	Buckling and post-buckling of FG-sandwich plates	Reddy's TSDT and von Kármán assumptions	Eigenvalue analysis and pseudo arc-length and Newton–Raphson	Critical loads and post-buckling paths highly dependent on porosity, GPL distribution, core-to face thickness ratio.
[197]	Static/dynamic snap-through of FG circular nanoplates	NET and von Kármán nonlinearity	Chebyshev–Ritz and Newmark and Budiansky-Roth	Imperfections, gradient index, and boundary conditions strongly affect static/dynamic snap-through.
[198]	Nonlinear post-buckling of porous circular nanoplates	Gurtin–Murdoch surface elasticity	Shooting method	Surface elastic modulus and residual stresses critically influence post-buckling and yield strength.
[199]	Nonlinear buckling and post-buckling of FG circular shallow arches	Geometric nonlinear theory	Analytical solution	Snap-through and post-buckling depend strongly on FG index, slenderness ratio, and modulus ratio.
[200]	Thermal buckling and post-buckling of FG nanobeams	TSDT	Jacobi–Ritz and Newton–Raphson	Layered vs. smooth GPL distributions alter results; differences reduce with more layers.
[201]	Thermal and mechanical post-buckling of truncated conical shells	Classical shell theory and nonlinear stress–strain	Galerkin method	Helical stiffener patterns offer best thermal buckling resistance; imperfections strongly affect response.
[202]	Buckling of nano-rod with surface effect	Gurtin–Murdoch and Steigmann–Ogden surface elasticity	Ritz method with Euler–Bernoulli and Timoshenko beam models	Surface effects and chosen elasticity model significantly alter critical load predictions.
[203]	Electro-mechanical buckling of flexoelectric cylindrical nanoshells	Flexoelectricity and HSDT	Galerkin's method with new displacement functions; nonlinear pre-buckling considered	Size-dependent critical stresses and buckling modes obtained. Boundary conditions, geometry, and applied electric voltage strongly affect stability. Pre-buckling deformation improves accuracy vs. linear theory.
[204]	Thermal buckling of magneto-electro-elastic (MEE) sandwich nanoplates with hexachiral auxetic core	NSGT and HSDT	Hamilton's principle; derived motion equations including MEE effects	Auxetic hexachiral core enhances thermal buckling resistance. Electric potential softens (reduces buckling temp); magnetic field hardens (increases stability). Useful for aerospace and sensor applications.

In addition to nonlocal and strain gradient models, surface elasticity has also been shown to play an important role in nanoscale buckling behavior. Bochkarev et al. [209] analyzed the buckling of nanoplates with a nanohole using a simplified version of the Gurtin–Murdoch surface elasticity model, in which only residual surface stresses were considered. In a subsequent study, Grekov and Bochkarev [210] employed the complete Gurtin–Murdoch formulation that includes both surface stress and surface elastic moduli, as well as full coupling between surface and bulk deformations. Their numerical results indicated that the complete model predicts approximately 30% higher critical buckling loads than the simplified formulation, particularly for plates thinner than 10 nm. In another

paper, Wang and Li [211] analyzed the buckling of nanotubes under uniaxial compression using a modified Euler model coupled with the Gurtin–Murdoch surface elasticity theory. Their formulation accounted for both inner and outer surface layers with independent surface stresses and surface elastic moduli, which were incorporated into the effective bending stiffness. They revealed that as the wall thickness decreases to the nanometer scale, surface effects significantly enhance the critical buckling load, producing a clear size-dependent stiffening behavior. They also showed that surface elasticity is mainly governed by nanotube geometry, while surface stress depends, additionally, on length and boundary conditions, with the predictions agreeing well with molecular-mechanics simulations.

Overall, these studies show that nanomechanics theories allow researchers to explore how small-scale effects influence buckling/post-buckling response. By changing parameters such as the nonlocal coefficient, gradient length scale, and geometry ratios, they can explain why nanoscale structures often behave stiffer or softer than predicted by classical elasticity. Table 8 summarizes how various nanomechanics theories change the critical buckling load of nanobeams, nanoplates, and cylindrical nanoshells compared with the classical model.

Table 8. Overall comparison of buckling behavior in different nanomechanics theories.

Structure	Nonlocal Elasticity	Strain Gradient	Couple Stress	Nonlocal–Gradient
Nanobeam	Decreases critical buckling load	Increases critical buckling load	Increases critical buckling load	Variable (depends on parameters)
Nanoplate	Decreases critical buckling load	Increases critical buckling load (stiffening)	Increases critical buckling load	Variable (depends on parameters)
Cylindrical shell	Decreases critical buckling load	Increases critical buckling load	Increases critical buckling load	Variable (depends on parameters)

5.3. Vibration and Dynamics Analyses

Dynamic analyses of nanostructures are often focused on CNT/NEMS resonators, nanobeams, and graphene membranes. Both free and forced vibrations, as well as nonlinear oscillations, are studied within the framework of nonlocal and strain gradient elasticity, combined with nonlinear beam and shell kinematics and viscoelastic damping models. Computational methods include modal finite element analysis, spectral methods, harmonic balance, reduced-order modeling, and MD. Findings indicate that natural frequencies decrease with increasing nonlocal effects, while nonlinear responses show either hardening or softening behaviors depending on geometry and boundary conditions. Resonance peaks and nonlinear dynamics are particularly significant for the development of high-frequency, ultra-sensitive NEMS resonators and energy-harvesting devices. In relation to vibration/dynamic analyses of nanostructures, several papers have been published recently. Alrubea and Abouelregal [212] studied the thermoelastic dynamics of viscoelastic nanobeams resting on Winkler elastic foundations under multiphysics interactions. They used modified Klein–Gordon nonlocal elasticity theory that accounted for both spatial and temporal nonlocality, combined with Tzou's dual-phase-lag heat conduction model and the Kelvin–Voigt viscoelastic model. The governing equations were derived from Hamilton's principle and solved via Laplace transforms and numerical inversion. Their results showed that spatial and temporal nonlocal parameters significantly reduced deflections, displacements, temperatures, and bending moments by redistributing stresses and incorporating memory effects. Increasing the Winkler foundation stiffness enhanced stability and reduced deformation, while viscoelastic damping coefficients controlled the vibration amplitudes. The study provided a comprehensive model capturing coupled thermoelastic–viscoelastic

behaviors at the nanoscale, offering insights for the design of MEMS/NEMS devices, sensors, and actuators operating under complex thermal and mechanical conditions.

Sur et al. [213] studied a dual-scale nonlocal strain gradient thermoelastic model that combined Eringen's spatial nonlocal elasticity with Klein–Gordon-type memory-dependent thermoelasticity within the Moore–Gibson–Thompson (MGT) framework. This formulation captures both spatial nonlocality and temporal memory effects, allowing accurate prediction of size-dependent vibration and thermal damping behavior in piezo-thermoelastic microbeams. The study provides an important link between nonlocal elasticity, strain gradient theory, and memory-based formulations, offering a more comprehensive description of nanoscale dynamic responses under multiphysical environments.

Ren and Qing [214] studied the buckling and vibration of FG magneto-electro-thermoelastic Timoshenko nanobeams using a general stress-driven two-phase local/nonlocal integral model and DQM. They noticed that increasing the nonlocal length scale reduced critical buckling loads and natural frequencies, whereas raising the local volume fraction produced the opposite effect. They also observed that the influence of the grading index reduced for high values, and sensitivity to nonlocal parameters increased with higher buckling modes. Das et al. [215] investigated the dynamics of FG nanobeams resting on a nonlocal elastic foundation using a nonlocal elasticity theory and using a semi-analytical eigenvalue approach. Their results showed that the consideration of nonlocal parameters introduced size-dependent softening effects, reducing natural frequencies and changing dynamic responses. The influence of material gradation, foundation stiffness, and beam geometry was also highlighted, demonstrating their combined impact on vibration characteristics and the stability of nanobeams. Koç et al. [216] studied the thermal and mechanical vibration behavior of sandwich nanoplates with auxetic cores and magneto-electro-elastic face layers using sinusoidal HSDT combined with NSGT. The results showed that auxetic cores improved stiffness and vibration resistance. Also, thermal gradients and magnetic potentials shifted natural frequencies and influenced vibration amplitudes. The study emphasized that tuning core geometry and face layer properties could optimize performance for aerospace and smart material applications. Zou and Kiani [217] studied the free vibration of FG graphene-reinforced composite nanoplates using a nonlocal quasi-3D plate model with the Navier method. The results showed that adding graphene platelets increased natural frequencies, and the FG-X distribution pattern led to the highest values. Increasing the nonlocal parameter reduced frequencies. Cuong-Le et al. [218] studied static bending and free-vibration laminated composite nanoplates using the Carrera unified formulation together with IGA and Eringen's NET. The findings showed that increasing the nonlocal parameter reduced stiffness and natural frequencies, while the length-to-thickness ratio, boundary conditions, and Young's modulus ratio had a strong impact on both static and vibration responses. Hoan et al. [219] studied the nonlinear vibration of nanobeams in a thermal environment while considering flexomagnetic effects and using NET. The governing equations were reduced with a yin-yang weighted averaging method, which allowed closed-form expressions for oscillation frequencies. The results showed that increasing temperature lowered vibration frequencies, while flexomagnetic coupling provided additional stiffness. Binh et al. [220] investigated the vibration response of nanobeams subjected to random loads in the presence of temperature, moisture, and flexoelectric effects, supported by viscoelastic foundations, using an analytical model that combined classical beam theory with NSGT. The findings indicated that flexoelectric effects reduced displacement amplitudes, whereas thermal and moisture conditions amplified them. Increasing the stiffness of the elastic foundation raised the frequencies, and viscous damping in the foundation limited oscillation amplitudes. They also observed that size-dependent effects led to frequency reductions more significantly compared with

predictions from classical theory. The authors of Ref. [221] examined the vibration of Euler–Bernoulli nanobeams subjected to gradient-type heating and a static magnetic field while considering nonlocal elasticity and thermoelasticity and using the Laplace transform with Riemann-sum inversion. The results showed that an increasing nonlocal parameter reduced stiffness, leading to higher deflections and displacements, though the effect on temperature was negligible. Herisanu et al. [222] investigated nonlinear longitudinal transverse vibrations of FG nanobeams under the combined action of mechanical impact and symmetric electromagnetic loading using the Galerkin Bubnov approach, while the optimal auxiliary functions method was employed to derive accurate analytical approximations close to resonance. The analysis was supported by stability checks using expansion methods, Routh–Hurwitz criteria, and Lyapunov functions, and results were compared with Runge–Kutta simulations. The study showed that nonlocal parameters reduced effective stiffness and lowered frequencies, while voltage-related parameters could either increase or decrease frequencies depending on their direction of influence. Zhang and Yang [223] investigated the vibration of piezoelectric nanobeams carrying an attached nanoparticle mass while considering flexoelectric and piezoelectric effects. The study showed that flexoelectricity significantly reduced resonance frequencies at small beam thicknesses, while piezoelectric effects modified the frequencies through induced axial forces that increased or decreased values depending on the applied voltage. Numerical examples indicated that resonance frequencies reduced rapidly with decreasing thickness. Also, they saw that the attached mass lowered frequencies for symmetric modes but had no effect on antisymmetric modes. Uzun et al. [224] studied the torsional vibration behavior of restrained non-circular nanowires embedded in an elastic medium and subjected to magnetic fields using NSGT. The warping of non-circular sections was included using Fourier series and Stokes' transform, which led to a general eigenvalue solution. The results showed that both nonlocal and strain gradient parameters strongly affected natural frequencies, with increasing nonlocal length scales reducing frequencies while larger strain gradient parameters raised them. Kadıoglu and Yaylı [225] investigated the torsional vibration of FG viscoelastic nanotubes under viscoelastic boundary conditions using doublet mechanics theory. This approach allowed them to couple nanoscale effects with damping behavior and to obtain complex frequency solutions, where the real part represented vibration frequency and the imaginary part represented damping. The findings highlighted that classical elastic models were inadequate for such systems, as damping effects at the nanoscale were significant. Kadioglu et al. [226] analyzed the torsional vibration of FG viscoelastic nanotubes with time-dependent boundary conditions based on NSGT. The equations of motion were derived using Hamilton's principle and the Kelvin–Voigt viscoelastic model, and they were solved with Fourier series expansions and Stokes' transform to obtain an eigenvalue problem. The study found that damping played a dominant role in vibration behavior. As nonlocal and power-law parameters increased, the effect of damping weakened, whereas higher strain gradient parameters amplified damping influence. Akpınar et al. [227] examined the torsional vibration of porous nanorods under arbitrary elastic boundary conditions by employing the nonlocal Lam strain gradient theory. The study showed that increasing the nonlocal parameter and porosity in shear modulus reduced torsional frequencies, while increasing material length-scale parameters, spring stiffness, and porosity in mass density raised them.

Li et al. [228] investigated the torsional vibration of imperfect multiwalled CNT (MWCNT) nanocomposite beams by considering reinforcement waviness, agglomeration, and porosity defects. The Halpin–Tsai model was modified to include these imperfections, and the governing equations were derived using the Hamiltonian approach within the Timoshenko–Gere beam theory. Analytical solutions showed that among beams with

different cross-sections, including rectangular, triangular, and elliptical shapes, rectangular cross-sections exhibited the highest torsional frequencies, while triangular ones had the lowest, which can be seen in Table 9. Table 9 presents frequency values for different porosity distributions, beam lengths, and MWCNTs' volume fractions (*C*–*C*, $e_0 = 0.2$, $a/b = 2$). As can be seen, increasing the porosity coefficient reduced natural frequencies due to the softening effect, and symmetry porosity distribution type-2 produced the largest frequency values; it should be noted in the uniform case, as the porosity is constant across the thickness, and in symmetry distribution-1, porosity is higher at the mid-plane and lower near the surfaces, meaning density is minimum at the center. Also, in symmetry distribution-2, porosity is higher near the surfaces and lower at the mid-plane, so density is at the maximum at the center. They expressed the effective material property (such as Young's modulus or density) as $P(x_3)$. It defines the function of the coordinate x_3 along the beam thickness. The coordinate x_3 varies from $-b$ to $+b$, where b denotes the half-thickness of the beam and $x_3 = 0$ corresponds to the mid-plane. Each porosity distribution pattern described as follows [228]:

$$\text{Uniform}: P(x_3) = P_1 e_2 \tag{20}$$

$$\text{Symmetric–1}: P(x_3) = P_1[1 - e_0 \cos(\frac{\pi x_3}{b})] \tag{21}$$

$$\text{Symmetric–2}: P(x_3) = P_1[1 - e_1(1 - \cos(\frac{\pi x_3}{b}))] \tag{22}$$

Table 9. Frequency values of porous MWCNT nanocomposite beam (with beam length = 0.3) [228].

Cross-Section	Porosity Distribution	Vfiber = 0	0.025	0.050	0.075
Elliptical	Uniform porosity distribution	7.7455	9.4250	10.1085	10.2965
	Symmetry porosity distribution-1	7.7515	9.4324	10.1163	10.3045
	Symmetry porosity distribution-2	7.7641	9.4477	10.1328	10.3213
Rectangular	Uniform porosity distribution	9.6823	11.7818	12.6361	12.8712
	Symmetry porosity distribution-1	9.6898	11.7909	12.6459	12.8812
	Symmetry porosity distribution-2	9.7055	11.8101	12.6665	12.9021
Triangular	Uniform porosity distribution	7.4994	9.1256	9.7873	9.9694
	Symmetry porosity distribution-1	7.5052	9.1327	9.7949	9.9772
	Symmetry porosity distribution-2	7.5174	9.1475	9.8109	9.9934

In the above equations, P_1 represents the material property of the nonporous (fully dense) nanocomposite, while e_0, e_1, and e_2 are porosity coefficients that determine the degree of porosity within the beam. These coefficients range between 0 and 1, and higher values correspond to greater porosity and, therefore, lower stiffness and density.

Uzun et al. [229] studied the torsional vibration of FG porous nanotubes using strain gradient elasticity to include size effects. The results showed that strain gradient parameters increased natural frequencies, while porosity reduced them. Compared with classical and CSTs, the model predicted higher frequencies, especially for higher modes. Authors of Ref. [197] analyzed axially moving nanobeams with harmonically varying length under thermal and mechanical loads using Euler–Bernoulli theory with nonlocal elasticity. Results showed that longer beams and higher temperatures increased instability, while greater thickness, axial tension, and stiffer foundations improved stability. Welles et al. [230] developed a theoretical model for the nonlinear dynamic analysis of nanoscale beams under intrinsic tension. Predictions matched experimental measurements for the first ten modes

of two nanoscale beams, confirming the model's validity for multimodal beam dynamics in nanoscale devices. Huang et al. [231] analyzed the dynamic stability of nanobeams by applying Reddy's higher-order beam theory together with Eringen's nonlocal elasticity. The results showed that increasing beam length shifted the instability region to lower frequencies and narrowed its width, while increasing height and Young's modulus also shifted it downward but widened the region. Also, they noticed the shear modulus had the opposite effect, moving the instability region upward. Moreover, they found that larger nonlocal parameters and higher density pushed the instability zones to lower frequencies. The foundation modulus had little effect on short beams but became more significant for longer beams, where it reduced stability.

Recent research has further expanded the understanding of the dynamic and vibrational behavior of single-walled CNTs (SWCNTs) under various physical conditions. Mohammed and Hussein [232] performed a nonlinear nonlocal torsional vibration of temperature-dependent viscoelastic SWCNTs in a viscoelastic medium with the Kelvin–Voigt model. Their results indicated that temperature and damping parameters have a significant effect on the torsional natural frequencies, providing valuable insights into the thermal and viscoelastic response of SWCNTs. Furthermore, Jayan et al. [233] investigated the vibration behavior of horn-shaped magneto-elastic SWCNTs conveying pulsating viscous fluid with the Haar wavelet method. The outcomes highlighted the importance of magnetic flux, Knudsen number, and viscous interaction in defining the vibrational stability of such nanostructures. These studies demonstrate the continuing progress in the numerical modeling and dynamic analysis of SWCNTs, particularly emphasizing their potential for sensing and nanoelectromechanical applications.

Summary of some studies concerning vibration and dynamic studies in nanomechanics can be seen in Table 10.

Table 10. Summary of some studies concerning vibration and dynamic studies in nanomechanics.

Ref.	Type of Analysis	Type of Theory	Numerical/Analytical Method	Key Findings
[234]	Free lateral vibration of short-fiber-reinforced and FG nanobeams	Stress-driven model (SDM), viscoelastic (Kelvin–Voigt)	Fourier sine series and Stokes transform	Nonlocal and boundary conditions significantly affect frequencies. Damping lowers vibrations.
[235]	Thermomechanical vibration of smart sandwich nanoplates	HSDT and NSGT	Analytical (Hamilton's principle, Navier approach)	Rising temperature softens materials, causes lower natural frequencies, and causes early buckling. Nonlocal effects change dynamic response.
[236]	Free vibration of GPL-reinforced porous double-curved shells of revolution	FSDT	Semi-analytical method (domain decomposition, MVP, Fourier and Chebyshev expansions)	Natural frequencies depend strongly on porosity, GPL distribution, and shell curvature. SAM matches FEM results, offering efficient accuracy.
[237]	Free vibration of graphene origami-reinforced cylindrical nanoshells	Shear deformable shell theory, Hamilton's principle	Analytical solution (Navier and Galerkin methods)	Frequencies increase with graphene origami fraction, decrease with thermal load, and with folding degree. Clamped–clamped BC yields highest frequencies. Origami design provides tunable vibration.
[238]	Free vibration of nanoframes considering shear deformation	NET and Timoshenko beam theory	Finite element (matrix displacement method)	Shear deformation lowers frequencies. Nonlocal parameter reduces them further, especially in thin frames. Mode sensitivity varies with size effects.
[239]	Free vibration of multiple-cracked FG nanostructures	NET and Timoshenko beam theory	Dynamic Stiffness Method (DSM)	Proposed exact DSM resolves nonlocal paradox in cantilever beams. Efficient computation of cracked FGM nanostructures. Crack severity, material gradation, and nonlocal effects strongly influence vibration.
[240]	Free vibration of piezoelectric nanobeams with surface and flexoelectric effects	Timoshenko and Euler–Bernoulli beam theories and flexoelectricity	Analytical (Navier method)	Dynamic flexoelectric effect has stronger size dependence than surface effect. Competing mechanisms change natural frequencies. Surface and flexoelectricity must be considered in nanoscale design.
[241]	Vibration analysis of CNTs as nanomechanical resonators	NET and Continuum mechanics	Analytical modeling	Resonant frequency decreases with axial force; nonlocal effects reduce stiffness, lowering resonance frequency. Results guide design of ultrasensitive CNT nanosensors.

Table 10. *Cont.*

Ref.	Type of Analysis	Type of Theory	Numerical/Analytical Method	Key Findings
[242]	Forced vibration of nanobeams under moving concentrated loads	Improved FSDT and Doublet Mechanics	Analytical solution and numerical simulation	Incorporating length scale increases stiffness, reduces deflection. Moving load velocity strongly affects peak amplification. Matches MD results.
[243]	Deterministic and stochastic free vibration of CNT-reinforced FGM cantilever plates	FSDT	FEM and Monte Carlo Simulation	Natural frequencies influenced by CNT distribution, thickness, power-law index, and temperature. Stochastic analysis shows dispersion sensitivity.
[244]	Steady-state vibration of GPL-reinforced beams with discontinuities	Euler–Lagrange formulation and micromechanical Halpin-Tsai/Voigt–Reuss	Fourier series and Cholesky method	Discontinuities and GPL distribution cause coupled axial–torsional–transverse vibrations. Natural frequencies shift due to cracks and filler percentages.
[245]	Free vibration of CNT-reinforced nanowires/nanobeams with movable ends	MCST	Fourier sine series and Stokes' transform	Movable boundary conditions strongly influence frequencies. CNT distribution, volume fraction, and rotary inertia significantly affect dynamic response.
[246]	Free vibration of viscoelastic nano-disks	MCST and the Zener viscoelastic model	Hamilton's principle, and Galerkin method, and Laplace transform	Viscoelastic damping lowers real and imaginary parts of eigenfrequencies. Size effects are more important at small h/l ratios. Boundary conditions alter responses.
[247]	Free vibration of multiple-cracked FGM nanostructures	NET and Timoshenko beam theory	Dynamic Stiffness Method (DSM)	Proposed exact DSM resolves nonlocal paradox in cracked FGMs. Crack depth, position, and gradation strongly affect frequencies.
[248]	Free vibration of axially FG Timoshenko nanobeams	Stress-driven two-phase local/nonlocal integral model	IGA using NURBS-based FEM	Nonlocal parameter, AFG index, and length-to-height ratio significantly affect vibration.
[249]	Free vibration of FG nanobeams with surface effects	Surface stress-driven nonlocal model and Bernoulli–Euler beam theory	Hamilton's principle with analytical modeling	Surface elasticity, residual stress, and density strongly influence vibration; model captures surface energy effects and provides design tool.
[250]	Forced vibration of Timoshenko nanobeam under accelerating moving load	NET (size-dependent)	Laplace transform analytical solution	Provides first exact solution for accelerated moving force; acceleration, deceleration, and nonlocal parameters alter deflection and transient response.
[251]	Mathematical modeling and vibration analysis of rotating FG porous spacecraft shafts reinforced with GPLs	Euler–Bernoulli beam theory and Kirchhoff plate theory	Assumed modes and Substructure modal synthesis	Rotation speed, GPL content/distribution, porosity patterns, and support conditions greatly influence vibration; enhancing spacecraft shaft design.
[252]	Nonlinear dynamic responses of FG porous beams	Reddy's HSDT	New semi-analytical approach (Galerkin method and perturbation technique)	Porosity distributions and gradation indexes significantly affect nonlinear vibrations. Semi-analytical method is efficient for dynamic response prediction.
[253]	Forced dynamics of elastically connected nano-plates and nano-shells	NET and Kirchhoff–Love plate theory and Novozhilov shallow shell theory	Coupled PDE system solved by modal analysis	Developed novel ECSNPS model. Nonlocal parameter, curvature, damping, and external excitation strongly influence vibration amplitudes. Useful for nano-sensors adaptable to curved surfaces.

6. Machine Learning (ML) Applications in Nanomechanics

Recent advances in ML have provided powerful tools for modeling and analysis in nanomechanics and nanostructured materials. Traditional numerical and analytical approaches, while accurate, often become computationally expensive when accounting for nanoscale effects or complex geometries. ML offers efficient alternatives by learning complex nonlinear relationships directly from data, enabling rapid prediction of important mechanical behaviors such as the vibration, buckling, bending, and thermal responses of nanostructures. Using ML techniques with continuum theories and multiscale simulations has emerged as a suitable strategy to accelerate the design, optimization, and characterization of nanosystems.

In Ref. [254], an ML framework was employed to predict the natural vibration frequencies of FG porous nanobeams. The input variables for the ML models consisted of four key physical parameters that significantly influenced the dynamic response of nanobeams, including the porosity coefficient associated with the elastic modulus (e_s), the porosity coefficient related to mass density (e_m), the temperature change (ΔT), and the nonlocal parameter (μ), which accounts for small-scale effects inherent in nanostructures. A comprehensive dataset was generated using the Sobol quasi-random sampling technique,

where each unique combination of these input parameters was analyzed with a nonlocal Levinson beam model for obtaining the natural frequencies. These computed frequencies, representing the first four vibration modes (f_1, f_2, f_3, f_4), served as the output targets for the ML algorithms. Four supervised regression models (artificial neural network (ANN), support vector regression (SVR), decision tree regression (DTR), and extreme gradient boosting (XGB)) were trained and optimized using Bayesian optimization to make the mapping between the input parameters and the resulting vibration frequencies. The predictive performance of each model was evaluated using statistical metrics such as the coefficient of determination (R^2), mean absolute error (MAE), mean absolute percentage error (MAPE), and root mean square error (RMSE). Also, the results showed that the ANN and SVR models achieved superior accuracy, with R^2 values approaching 0.999, which indicates excellent agreement between the ML predictions and the theoretical results. So, the proposed ML approach effectively approximates the complex numerical behavior of nonlocal nanobeams, which offers a fast and accurate alternative to traditional analytical or numerical methods for vibration analysis.

In Ref. [255], the buckling response of carbon nanotube-reinforced hybrid FG plates was investigated using a formulation based on modified TSDT. A C^0 finite element model was implemented in MATLAB R2023b to compute a dataset of critical buckling loads under different material parameters. These results were then used to train three ML models: a deep neural network, an extreme gradient boosting model (XGBoost), and a random forest. The input features consisted of effective material properties such as Young's modulus, Poisson's ratio, CNT volume fraction, and gradation index, while the output was the critical buckling load. The deep neural network employed a multilayer feedforward architecture trained via backpropagation, whereas XGBoost and random forest were ensemble tree-based methods trained on the same dataset. Once trained, these models were able to predict the buckling loads for new parameter sets with high accuracy, significantly reducing computational cost compared to repeated finite element simulations and demonstrating strong potential for efficient structural design and analysis.

In Ref. [256], the dynamic behavior of graphene nanocomposite beams subjected to thermal environments was investigated using a hybrid Galerkin–ML framework. A refined higher-order beam theory was derived from the Hamilton principle, and the Galerkin method was applied to obtain numerical solutions. The data generated from these simulations included beam aspect ratios, temperature variations, and graphene platelet weight fractions as input parameters, with the fundamental natural frequency as the output. The data was used to train three regression models, such as polynomial regression, support vector regression, and random forest regression. The polynomial regression model showed the nonlinear relationships between the inputs better and gave the lowest error, performing better than the other models. The combined Galerkin–ML strategy provided accurate predictions of natural frequencies while significantly reducing computational effort compared to purely numerical approaches.

In Ref. [257], attention was directed toward predicting nonlocal elasticity parameters of nanostructures such as CNTs and boron nitride nanotubes. The theoretical foundation was based on the modified strain gradient theory, while extensive MD simulations were carried out to generate training data for different loading conditions, including compression, tension, and bending. ML models (such as Gaussian process regression, support vector machines, and neural networks) were trained on the MD results. These models enabled accurate and rapid estimation of length-scale parameters, thereby reducing the reliance on computationally expensive atomistic simulations.

The authors of Ref. [258] studied the experimental characterization of GPLs. Raman spectroscopy was employed to collect spectral data, which was then analyzed with numeri-

cal peak-fitting techniques and advanced ML algorithms. Traditional classifiers were tested alongside a convolutional neural network, the latter achieving classification accuracies of up to 86 percent. This method was fast and low-cost for checking the quality of GPLs during production. Also, it helped solve an important problem in the industrial processing of two-dimensional materials. In Ref. [259], the bending analysis of nanoplates using strain gradient elasticity theory was examined. The governing equations, which became sixth-order partial differential equations due to size effects, were traditionally difficult to solve using finite elements or analytical approaches. To address this, authors employed physics-informed neural networks (PINNs), where the PDEs were directly embedded into the loss function during training. The network takes spatial coordinates as inputs and predicts the transverse displacement field as the output, thus bypassing the need for FEM or experimental data generation. Training was performed using the extreme learning machine (ELM) algorithm, in which hidden layer weights and biases were initialized randomly and kept fixed, while the output weights were obtained through a least-squares solution. This training strategy ensured much faster convergence compared to gradient descent. The same framework was applied to both direct problems, where the flexural response was computed, and inverse problems, where the internal nonlocal length-scale parameters were identified from noisy measurements. The results demonstrated excellent agreement with analytical and FEM solutions, with small errors, highlighting the efficiency and accuracy of the proposed PINN–ELM approach for nanoscale bending analysis.

Taken together, these studies illustrated different ways in which advanced theories, numerical techniques, and ML frameworks had been used for the analysis and characterization of nanostructures. A wide range of ML techniques (including deep neural networks, ensemble methods, support vector machines, Gaussian process regression, convolutional neural networks, and physics-informed neural networks) were successfully applied. Overall, these approaches demonstrated improvements in computational efficiency, predictive accuracy, and experimental validation and opened new ways for the design and characterization of next-generation nanomaterials.

7. Conclusions

This review summarizes the main theories and computational methods used in nanomechanics for analyzing nanostructures, focusing on the most recent studies published in the past few years. Classical continuum models cannot describe size effects and surface interactions at the nanoscale, so advanced theories such as nonlocal elasticity, strain gradient, couple stress, and surface elasticity theories have been developed. Numerical approaches, including FEM, DQM, Galerkin, mesh-free, and peridynamic methods, have been chosen to solve these models. Using nanomaterials in MEMS/NEMS has expanded their applications in sensing, actuation, and energy systems.

Recently, machine learning techniques have enabled faster and more accurate prediction of nanoscale behaviors, offering efficient alternatives to traditional methods. For example, ML models demonstrate high accuracy in predicting natural frequencies of nanostructures. Moreover, the ML approach effectively approximates the complex numerical behavior of nanostructures, which offers a fast and accurate alternative to traditional analytical or numerical methods.

Combining advanced theories, numerical models, and data-driven approaches provides a strong foundation for future research and the design of next-generation nanoengineering materials and devices.

Although many theories have been proposed to describe the size-dependent behavior of nanostructures, the main theoretical challenge is still to develop a general model that can be confirmed by experiments. Most of the existing nonlocal, strain gradient, and

surface elasticity theories use parameters that are difficult to measure and do not have a clear physical meaning. In addition, the overlap between these theories sometimes causes confusion and limits their ability to make accurate predictions. Future studies should, therefore, focus on building a consistent multiscale model that connects atomic-level behavior with continuum mechanics in a reliable and practical way.

Author Contributions: M.S.: Conceptualization, methodology, writing—review and editing, software, validation, formal analysis, investigation, and writing—original draft preparation. A.P.: Supervision, conceptualization, visualization, project administration, methodology, and formal analysis. G.J.: Data curation, writing—review and editing, validation, and investigation. All authors have read and agreed to the published version of the manuscript.

Funding: This research received no external funding.

Data Availability Statement: No new data were created or analyzed in this study.

Conflicts of Interest: The authors declare no conflicts of interest.

References

1. Nasrollahzadeh, M.; Sajadi, S.M.; Sajjadi, M.; Issaabadi, Z. An Introduction to Nanotechnology. In *Interface Science and Technology*; Nasrollahzadeh, M., Sajadi, S.M., Sajjadi, M., Issaabadi, Z., Atarod, M., Eds.; Elsevier: Amsterdam, The Netherlands, 2019; Chapter 1; Volume 28, pp. 1–27.
2. Blandón-González, B.; Trompeta, A.F.; Mercader-Moyano, P. Advanced materials: Introduction to nanotechnology. In *Life Cycle Analysis Based on Nanoparticles Applied to the Construction Industry: A Comprehensive Curriculum*; Mercader-Moyano, P., Porras-Pereira, P., Eds.; Springer Nature: Cham, Switzerland, 2025; pp. 61–73.
3. Kumari, S.; Raturi, S.; Kulshrestha, S.; Chauhan, K.; Dhingra, S.; András, K.; Thu, K.; Khargotra, R.; Singh, T. A comprehensive review on various techniques used for synthesizing nanoparticles. *J. Mater. Res. Technol.* **2023**, *27*, 1739–1763. [CrossRef]
4. Roudbari, M.A.; Jorshari, T.D.; Lü, C.; Ansari, R.; Kouzani, A.Z.; Amabili, M. A review of size-dependent continuum mechanics models for micro- and nano-structures. *Thin-Walled Struct.* **2022**, *170*, 108562. [CrossRef]
5. Eringen, A.C. On differential equations of nonlocal elasticity and solutions of screw dislocation and surface waves. *J. Appl. Phys.* **1983**, *54*, 4703–4710. [CrossRef]
6. Mindlin, R.D. Micro-structure in linear elasticity. *Arch. Ration. Mech. Anal.* **1964**, *16*, 51–78. [CrossRef]
7. Fleck, N.A.; Hutchinson, J.W. A reformulation of strain gradient plasticity. *J. Mech. Phys. Solids* **2001**, *49*, 2245–2271. [CrossRef]
8. Yan, Z.; Jiang, L. Modified Continuum Mechanics Modeling on Size-Dependent Properties of Piezoelectric Nanomaterials: A Review. *Nanomaterials* **2017**, *7*, 27. [CrossRef]
9. Yang, F.; Chong, A.C.M.; Lam, D.C.C.; Tong, P. Couple stress based strain gradient theory for elasticity. *Int. J. Solids Struct.* **2002**, *39*, 2731–2743. [CrossRef]
10. Gurtin, M.E.; Ian Murdoch, A. A continuum theory of elastic material surfaces. *Arch. Ration. Mech. Anal.* **1975**, *57*, 291–323. [CrossRef]
11. Silling, S.A. Reformulation of elasticity theory for discontinuities and long-range forces. *J. Mech. Phys. Solids* **2000**, *48*, 175–209. [CrossRef]
12. Braides, A.; Causin, A.; Solci, M.; Truskinovsky, L. Beyond the Classical Cauchy–Born Rule. *Arch. Ration. Mech. Anal.* **2023**, *247*, 107. [CrossRef]
13. Tadmor, E.B.; Ortiz, M.; Phillips, R. Quasicontinuum analysis of defects in solids. *Philos. Mag. A* **1996**, *73*, 1529–1563. [CrossRef]
14. Barretta, R.; Marotti de Sciarra, F.; Vaccaro, M.S. Nonlocal Elasticity for Nanostructures: A Review of Recent Achievements. *Encyclopedia* **2023**, *3*, 279–310. [CrossRef]
15. Eltaher, M.A.; Khater, M.E.; Emam, S.A. A review on nonlocal elastic models for bending, buckling, vibrations, and wave propagation of nanoscale beams. *Appl. Math. Model.* **2016**, *40*, 4109–4128. [CrossRef]
16. Thai, H.-T.; Vo, T.P.; Nguyen, T.-K.; Kim, S.-E. A review of continuum mechanics models for size-dependent analysis of beams and plates. *Compos. Struct.* **2017**, *177*, 196–219. [CrossRef]
17. Farajpour, A.; Ghayesh, M.H.; Farokhi, H. A review on the mechanics of nanostructures. *Int. J. Eng. Sci.* **2018**, *133*, 231–263. [CrossRef]
18. Ghayesh, M.H.; Farajpour, A. A review on the mechanics of functionally graded nanoscale and microscale structures. *Int. J. Eng. Sci.* **2019**, *137*, 8–36. [CrossRef]
19. Nuhu, A.A.; Safaei, B. A comprehensive review on the vibration analyses of small-scaled plate-based structures by utilizing the nonclassical continuum elasticity theories. *Thin-Walled Struct.* **2022**, *179*, 109622. [CrossRef]

20. Khaniki, H.B.; Ghayesh, M.H.; Amabili, M. A review on the statics and dynamics of electrically actuated nano and micro structures. *Int. J. Non-Linear Mech.* **2021**, *129*, 103658. [CrossRef]
21. Yee, K.; Ghayesh, M.H. A review on the mechanics of graphene nanoplatelets reinforced structures. *Int. J. Eng. Sci.* **2023**, *186*, 103831. [CrossRef]
22. Imani Yengejeh, S.; Kazemi, S.A.; Öchsner, A. Advances in mechanical analysis of structurally and atomically modified carbon nanotubes and degenerated nanostructures: A review. *Compos. Part B Eng.* **2016**, *86*, 95–107. [CrossRef]
23. Soni, S.K.; Thomas, B.; Swain, A.; Roy, T. Functionally graded carbon nanotubes reinforced composite structures: An extensive review. *Compos. Struct.* **2022**, *299*, 116075. [CrossRef]
24. Sayyad, A.S.; Hadji, L.; Tounsi, A. On the mechanics of FG nanobeams: A review with numerical analysis. *Forces Mech.* **2023**, *12*, 100219. [CrossRef]
25. Qin, Q. Research Progress and Applications of Carbon Nanotubes, Black Phosphorus, and Graphene-Based Nanomaterials: Insights from Computational Simulations. *Comput. Mater. Contin.* **2025**, *85*, 1–39. [CrossRef]
26. Torkaman-Asadi, M.A.; Kouchakzadeh, M.A. Atomistic simulations of mechanical properties and fracture of graphene: A review. *Comput. Mater. Sci.* **2022**, *210*, 111457. [CrossRef]
27. Chandel, V.S.; Wang, G.; Talha, M. Advances in modelling and analysis of nano structures: A review. *Nanotechnol. Rev.* **2020**, *9*, 230–258. [CrossRef]
28. Xu, D.; Xu, J.; Xiong, S.; Chen, L.; He, Q.; Wang, B.; Li, R. Hamiltonian system-based analytic thermal buckling solutions of orthotropic rectangular plates. *Int. J. Mech. Sci.* **2024**, *267*, 108987. [CrossRef]
29. Zheng, X.; Huang, M.; An, D.; Zhou, C.; Li, R. New analytic bending, buckling, and free vibration solutions of rectangular nanoplates by the symplectic superposition method. *Sci. Rep.* **2021**, *11*, 2939. [CrossRef]
30. Singh, P.P.; Azam, M.S. Free vibration and buckling analysis of elastically supported transversely inhomogeneous functionally graded nanoplate in thermal environment using Rayleigh–Ritz method. *J. Vib. Control* **2020**, *27*, 2835–2847. [CrossRef]
31. Karami, B.; Janghorban, M.; Tounsi, A. Galerkin's approach for buckling analysis of functionally graded anisotropic nanoplates/different boundary conditions. *Eng. Comput.* **2019**, *35*, 1297–1316. [CrossRef]
32. Li, Y.-D.; Tang, Z.-C.; Fu, Z.-J. Generalized Finite Difference Method for Plate Bending Analysis of Functionally Graded Materials. *Mathematics* **2020**, *8*, 1940. [CrossRef]
33. Malekzadeh, P.; Shojaee, M. A two-variable first-order shear deformation theory coupled with surface and nonlocal effects for free vibration of nanoplates. *J. Vib. Control* **2013**, *21*, 2755–2772. [CrossRef]
34. Belarbi, M.-O.; Benounas, S.; Li, L.; Van Vinh, P.; Garg, A. Vibration of a Functionally Graded Doubly Curved Shallow Nanoshell: An Improved FSDT Model and its Nonlocal Finite Element Implement. *J. Vib. Eng. Technol.* **2025**, *13*, 93. [CrossRef]
35. Bian, P.-L.; Qing, H. Structural analysis of nonlocal nanobeam via FEM using equivalent nonlocal differential model. *Eng. Comput.* **2023**, *39*, 2565–2581. [CrossRef]
36. Le, T.S.; Dang, H.T.; Tran, T.T.; Du, N.V.; Luong, H.G.; Pham, Q.H. Isogeometric free vibration analysis of tri-directional functionally graded nanoplates based on non-local elasticity theory. *J. Braz. Soc. Mech. Sci. Eng.* **2025**, *47*, 263. [CrossRef]
37. Le, H.Q.; Khatir, S.; Cuong-Le, T. NURBS-based isogeometric analysis for layerwise local behavior of nano-laminated plates based on refined zigzag and nonlocal strain gradient theories. *Compos. Struct.* **2025**, *354*, 118766. [CrossRef]
38. Abdoh, D.A.; Yin, B.B.; Kodur, V.K.R.; Liew, K.M. Computationally efficient and effective peridynamic model for cracks and fractures in homogeneous and heterogeneous materials. *Comput. Methods Appl. Mech. Eng.* **2022**, *399*, 115318. [CrossRef]
39. Zhao, D.; Wang, J.; Xu, Z. Surface Effect on Vibration of Timoshenko Nanobeam Based on Generalized Differential Quadrature Method and Molecular Dynamics Simulation. *Nano Manuf. Metrol.* **2021**, *4*, 298–313. [CrossRef]
40. Latif, A.; Latif, A.; Mohsin, M.; Bhatti, I.A. Density functional theory for nanomaterials: Structural and spectroscopic applications—A review. *J. Mol. Model.* **2025**, *31*, 211. [CrossRef]
41. Zhang, Z.; Wang, C.; Hu, X.; Ni, Y. Shape Effect of Surface Defects on Nanohardness by Quasicontinuum Method. *Micromachines* **2020**, *11*, 909. [CrossRef]
42. Xia, C.; Xu, W.; Nie, G. Dynamic quasi-continuum model for plate-type nano-materials and analysis of fundamental frequency. *Appl. Math. Mech.* **2021**, *42*, 85–94. [CrossRef]
43. Hughes, K.J.; Iyer, K.A.; Bird, R.E.; Ivanov, J.; Banerjee, S.; Georges, G.; Zhou, Q.A. Review of Carbon Nanotube Research and Development: Materials and Emerging Applications. *ACS Appl. Nano Mater.* **2024**, *7*, 18695–18713. [CrossRef]
44. Li, Q.; Niu, X.; Pan, Z.; Zhang, J. Nonlinear buckling and post-buckling of multilayered piezoelectric graded porous circular nanoplates considering of surface/interface effects. *Thin-Walled Struct.* **2025**, *212*, 113236. [CrossRef]
45. Akpınar, M.; Kafkas, U.; Uzun, B.; Yaylı, M.Ö. Size-dependent longitudinal vibration of embedded FG Bishop nanotubes by incorporating deformable boundary conditions. *Int. J. Mech. Mater. Des.* **2025**. [CrossRef]
46. Kadioglu, H.G.; Yayli, M.O. Axial Vibration of a Viscoelastic FG Nanobeam with Arbitrary Boundary Conditions. *J. Vib. Eng. Technol.* **2025**, *13*, 96. [CrossRef]

47. Yayli, M.Ö. Buckling analysis of a microbeam embedded in an elastic medium with deformable boundary conditions. *Micro Nano Lett.* **2016**, *11*, 741–745. [CrossRef]
48. Yayli, M.Ö. Axial vibration analysis of a Rayleigh nanorod with deformable boundaries. *Microsyst. Technol.* **2020**, *26*, 2661–2671. [CrossRef]
49. Darban, H. MD benchmarks: Size-dependent tension, bending, buckling, and vibration of nanobeams. *Int. J. Mech. Sci.* **2025**, *296*, 110316. [CrossRef]
50. Civalek, Ö.; Uzun, B.; Yaylı, M.Ö. Nonlocal Free Vibration of Embedded Short-Fiber-Reinforced Nano-/Micro-Rods with Deformable Boundary Conditions. *Materials* **2022**, *15*, 6803. [CrossRef]
51. Kafkas, U.; Uzun, B.; Yaylı, M.Ö.; Güçlü, G. Thermal vibration of perforated nanobeams with deformable boundary conditions via nonlocal strain gradient theory. *Z. Für Naturforschung Sect. A J. Phys. Sci.* **2023**, *78*, 681–701. [CrossRef]
52. Hutapea, J.A.; Manik, Y.G.; Ndruru, S.T.; Huang, J.; Goei, R.; Tok, A.I.; Siburian, R. Comprehensive Review of Graphene Synthesis Techniques: Advancements, Challenges, and Future Directions. *Micro* **2025**, *5*, 40. [CrossRef]
53. Ali, Z.; Yaqoob, S.; Yu, J.; D'Amore, A. Critical review on the characterization, preparation, and enhanced mechanical, thermal, and electrical properties of carbon nanotubes and their hybrid filler polymer composites for various applications. *Compos. Part C Open Access* **2024**, *13*, 100434. [CrossRef]
54. Gul, U.; Aydogdu, M. Longitudinal vibration of Bishop nanorods model based on nonlocal strain gradient theory. *J. Braz. Soc. Mech. Sci. Eng.* **2022**, *44*, 377. [CrossRef]
55. Juntarasaid, C.; Pulngern, T.; Chucheepsakul, S. A variational method for post-buckling analysis of end-supported nanorods under self-weight with surface stress effect. *Arch. Appl. Mech.* **2021**, *91*, 1021–1035. [CrossRef]
56. Uzun, B.; Kafkas, U.; Deliktaş, B.; Yaylı, M.Ö. Size-Dependent Vibration of Porous Bishop Nanorod with Arbitrary Boundary Conditions and Nonlocal Elasticity Effects. *J. Vib. Eng. Technol.* **2023**, *11*, 809–826. [CrossRef]
57. Prasittikulwat, S.; Pulngern, T.; Chucheepsakul, S.; Phungpaingam, B. Large Deflection and Post-Buckling Analysis of Cantilever Nanorods Including Effects of Couple and Surface Stresses by Intrinsic Coordinate Finite Elements. *Int. J. Struct. Stab. Dyn.* **2023**, *24*, 2450211. [CrossRef]
58. Juntarasaid, C.; Pulngern, T.; Chucheepsakul, S. Postbuckling Analysis of a Nonlocal Nanorod Under Self-Weight. *Int. J. Appl. Mech.* **2020**, *12*, 2050035. [CrossRef]
59. Ahmadi, I.; Sladek, V.; Sladek, J. Instability and buckling analysis of bi-directional FG multiple nanobeam system in thermal environment by a meshless method. *Arch. Appl. Mech.* **2025**, *95*, 181. [CrossRef]
60. Hamed, M.A.; Mohamed, N.A.; Eltaher, M.A. Stability buckling and bending of nanobeams including cutouts. *Eng. Comput.* **2022**, *38*, 209–230. [CrossRef]
61. Hosseini, S.A.H.; Rahmani, O. Surface Effects on Buckling of Double Nanobeam System Based on Nonlocal Timoshenko Model. *Int. J. Struct. Stab. Dyn.* **2016**, *16*, 1550077. [CrossRef]
62. Nazmul, I.M.; Devnath, I. Analytical buckling analysis of bidirectional functionally graded nonlocal nanobeams. *Int. J. Comput. Mater. Sci. Eng.* **2024**, *15*, 2450024. [CrossRef]
63. Yan, X.; Li, Y. Size-dependent buckling behaviors of a rotating nanobeam using the integral form of Eringen's nonlocal theory. *Mech. Adv. Mater. Struct.* **2024**, *31*, 5437–5453. [CrossRef]
64. Thang, P.T. Buckling analysis of graphene nanoplatelets/polymer composite sandwich cylindrical shells with auxetic honeycomb core under external pressure. *Mech. Based Des. Struct. Mach.* **2025**, *53*, 6722–6748. [CrossRef]
65. Wang, W.; Yin, H.; Zhang, J.; Sun, J.; Zhou, Z.; Xu, X. Nonlinear stability characteristics of piezoelectric cylindrical shells with flexoelectric effects. *Acta Mech. Sin.* **2024**, *41*, 424412. [CrossRef]
66. Avey, M.; Fantuzzi, N.; Sofiyev, A.H. Analytical Solution of Stability Problem of Nanocomposite Cylindrical Shells under Combined Loadings in Thermal Environments. *Mathematics* **2023**, *11*, 3781. [CrossRef]
67. Sofiyev, A.H. Modeling and solution of eigenvalue problems of laminated cylindrical shells consisting of nanocomposite plies in thermal environments. *Arch. Appl. Mech.* **2024**, *94*, 3071–3099. [CrossRef]
68. Shi, S.; Fan, X. Size-dependent thermoelastic dissipation and frequency shift in micro/nano cylindrical shell based on surface effect and dual-phase lag heat conduction model. *Acta Mech.* **2024**, *235*, 7855–7879. [CrossRef]
69. Zhou, H.; Jing, C.; Li, P. Generalized thermoelastic damping in micro/nano-ring resonators undergoing out-of-plane vibration. *Int. J. Mech. Sci.* **2024**, *278*, 109490. [CrossRef]
70. Wang, C.M.; Xiang, Y.; Yang, J.; Kitipornchai, S. Buckling of nano-rings/arches based on nonlocal elasticity. *Int. J. Appl. Mech.* **2012**, *4*, 1250025. [CrossRef]
71. Sadeghian, M.; Palevicius, A.; Janusas, G. Nonlocal Strain Gradient Model for the Nonlinear Static Analysis of a Circular/Annular Nanoplate. *Micromachines* **2023**, *14*, 1052. [CrossRef]
72. Duc, D.H.; Thom, D.V.; Cong, P.H.; Minh, P.V.; Nguyen, N.X. Vibration and static buckling behavior of variable thickness flexoelectric nanoplates. *Mech. Based Des. Struct. Mach.* **2023**, *51*, 7102–7130. [CrossRef]

73. Phuc, P.Q.; Van Dong, P.; Hai, N.T.; Thien, L.G. Forced vibration of composite nanoplates taking into the structural drag phenomenon. *Structures* **2025**, *75*, 108633. [CrossRef]
74. Eringen, A.C.; Edelen, D.G.B. On nonlocal elasticity. *Int. J. Eng. Sci.* **1972**, *10*, 233–248. [CrossRef]
75. Ceballes, S.; Larkin, K.; Rojas, E.; Ghaffari, S.S.; Abdelkefi, A. Nonlocal elasticity and boundary condition paradoxes: A review. *J. Nanoparticle Res.* **2021**, *23*, 66. [CrossRef]
76. Romano, G.; Barretta, R.; Diaco, M.; Marotti de Sciarra, F. Constitutive boundary conditions and paradoxes in nonlocal elastic nanobeams. *Int. J. Mech. Sci.* **2017**, *121*, 151–156. [CrossRef]
77. Kaplunov, J.; Prikazchikov, D.A.; Prikazchikova, L. On integral and differential formulations in nonlocal elasticity. *Eur. J. Mech. A/Solids* **2023**, *100*, 104497. [CrossRef]
78. Challamel, N.; Zhang, Z.; Wang, C.M.; Reddy, J.N.; Wang, Q.; Michelitsch, T.; Collet, B. On nonconservativeness of Eringen's nonlocal elasticity in beam mechanics: Correction from a discrete-based approach. *Arch. Appl. Mech.* **2014**, *84*, 1275–1292. [CrossRef]
79. Romano, G.; Barretta, R. Nonlocal elasticity in nanobeams: The stress-driven integral model. *Int. J. Eng. Sci.* **2017**, *115*, 14–27. [CrossRef]
80. Patnaik, S.; Sidhardh, S.; Semperlotti, F. Displacement-driven approach to nonlocal elasticity. *Eur. J. Mech. A/Solids* **2022**, *92*, 104434. [CrossRef]
81. Vaccaro, M.S.; Pinnola, F.P.; de Sciarra, F.M.; Barretta, R. Limit behaviour of Eringen's two-phase elastic beams. *Eur. J. Mech. -A/Solids* **2021**, *89*, 104315. [CrossRef]
82. Shaat, M. An iterative nonlocal residual constitutive model for nonlocal elasticity. *arXiv* **2018**, arXiv:1803.08646. [CrossRef]
83. Romano, G.; Diaco, M. On formulation of nonlocal elasticity problems. *Meccanica* **2021**, *56*, 1303–1328. [CrossRef]
84. Romano, G.; Barretta, R. Stress-driven versus strain-driven nonlocal integral model for elastic nano-beams. *Compos. Part B Eng.* **2017**, *114*, 184–188. [CrossRef]
85. Ding, W. Advancing Integral Nonlocal Elasticity via Fractional Calculus: Theory, Modeling, and Applications. Ph.D. Thesis, Purdue University Graduate School, West Lafayette, IN, USA, 2024.
86. Aifantis, E.C. Strain gradient interpretation of size effects. *Int. J. Fract.* **1999**, *95*, 299–314. [CrossRef]
87. Hosseini, M.; Dini, A.; Eftekhari, M. Strain gradient effects on the thermoelastic analysis of a functionally graded micro-rotating cylinder using generalized differential quadrature method. *Acta Mech.* **2017**, *228*, 1563–1580. [CrossRef]
88. Sadeghi, H.; Baghani, M.; Naghdabadi, R. Strain gradient elasticity solution for functionally graded micro-cylinders. *Int. J. Eng. Sci.* **2012**, *50*, 22–30. [CrossRef]
89. Wu, C.-P.; Chang, T.-Y. A Review of Modified/Consistent Couple Stress and Strain Gradient Theories for Analyzing Static and Dynamic Behaviors of Functionally Graded Microscale Plates and Shells. *Materials* **2025**, *18*, 4475. [CrossRef]
90. Kong, S. A Review on the Size-Dependent Models of Micro-beam and Micro-plate Based on the Modified Couple Stress Theory. *Arch. Comput. Methods Eng.* **2022**, *29*, 1–31. [CrossRef]
91. Hadjesfandiari, A.R.; Dargush, G.F. Couple stress theories: Theoretical underpinnings and practical aspects from a new energy perspective. *arXiv* **2016**, arXiv:1611.10249. [CrossRef]
92. Hadjesfandiari, A.R. The Character of Couples and Couple Stresses in Continuum Mechanics. *Symmetry* **2024**, *16*, 1046. [CrossRef]
93. Park, S.K.; Gao, X.L. Variational formulation of a modified couple stress theory and its application to a simple shear problem. *Z. Für Angew. Math. Phys.* **2008**, *59*, 904–917. [CrossRef]
94. Münch, I.; Neff, P.; Madeo, A.; Ghiba, I.D. The modified indeterminate couple stress model: Why Yang et al.'s arguments motivating a symmetric couple stress tensor contain a gap and why the couple stress tensor may be chosen symmetric nevertheless. *Z. Für Angew. Math. Mech.* **2017**, *97*, 1524–1554. [CrossRef]
95. Mohammad-Abadi, M.; Daneshmehr, A.R. Modified couple stress theory applied to dynamic analysis of composite laminated beams by considering different beam theories. *Int. J. Eng. Sci.* **2015**, *87*, 83–102. [CrossRef]
96. Hadjesfandiari, A.R.; Dargush, G.F. An Assessment of Couple Stress Theories. *Preprints* **2018**.
97. Trabelssi, M.; El-Borgi, S.; Friswell, M.I. Application of nonlocal strain gradient theory for the analysis of bandgap formation in metamaterial nanobeams. *Appl. Math. Model.* **2024**, *127*, 281–296. [CrossRef]
98. Zaera, R.; Serrano, Ó.; Fernández-Sáez, J. On the consistency of the nonlocal strain gradient elasticity. *Int. J. Eng. Sci.* **2019**, *138*, 65–81. [CrossRef]
99. Shaat, M. Infeasibility of the nonlocal strain gradient theory for applied physics. *arXiv* **2017**, arXiv:1711.09938. [CrossRef]
100. Barretta, R.; Faghidian, S.A.; Marotti de Sciarra, F.; Vaccaro, M.S. Nonlocal strain gradient torsion of elastic beams: Variational formulation and constitutive boundary conditions. *Arch. Appl. Mech.* **2020**, *90*, 691–706. [CrossRef]
101. Aifantis, E.C. A concise review of gradient models in mechanics and physics. *Front. Phys.* **2020**, *7*, 239. [CrossRef]

102. Gortsas, T.; Aggelis, D.G.; Polyzos, D. The strain gradient elasticity via nonlocal considerations. *Int. J. Solids Struct.* **2023**, *269*, 112177. [CrossRef]
103. Fonseca Gonçalves, G.; Rodrigues Lopes, I.A.; Couto Carneiro, A.M.; Andrade Pires, F.M. A critical comparison of gradient and integral nonlocal damage models: Formulation, numerical predictions and computational aspects. *Finite Elem. Anal. Des.* **2025**, *248*, 104358. [CrossRef]
104. Mogilevskaya, S.G.; Zemlyanova, A.Y.; Mantič, V. The use of the Gurtin-Murdoch theory for modeling mechanical processes in composites with two-dimensional reinforcements. *Compos. Sci. Technol.* **2021**, *210*, 108751. [CrossRef]
105. Hassanpour, S.; Heppler, G.R. Micropolar elasticity theory: A survey of linear isotropic equations, representative notations, and experimental investigations. *Math. Mech. Solids* **2015**, *22*, 224–242. [CrossRef]
106. Barbhuiya, S.; Jivkov, A.; Das, B.B. A review of multi-scale modelling of concrete deterioration: Fundamentals, techniques and perspectives. *Constr. Build. Mater.* **2023**, *406*, 133472. [CrossRef]
107. Phuc, P.Q.; Van Dong, P.; Hai, N.T.; Zenkour, A.M.; Thien, L.G. The application of novel shear deformation theory and nonlocal elasticity theory to study the mechanical response of composite nanoplates. *Compos. Struct.* **2025**, *352*, 118646. [CrossRef]
108. Li, S.; Cheng, Y. Study on wave dispersion behavior in an embedded triclinic microscale plate based on Eringen's nonlocal elasticity theory. *Mech. Based Des. Struct. Mach.* **2025**, 1–21. [CrossRef]
109. Siddique, M.U.M.; Nazmul, I.M. Static bending analysis of BDFG nanobeams by nonlocal couple stress theory and nonlocal strain gradient theory. *Forces Mech.* **2024**, *17*, 100289. [CrossRef]
110. Kong, L.; Zhang, B.; Li, C. Thermal Buckling and Postbuckling Behaviors of Couple Stress and Surface Energy-Enriched FG-CNTR Nanobeams. *Symmetry* **2022**, *14*, 2228. [CrossRef]
111. Togun, N.; Bağdatli, S.M. Application of Modified Couple-Stress Theory to Nonlinear Vibration Analysis of Nanobeam with Different Boundary Conditions. *J. Vib. Eng. Technol.* **2024**, *12*, 6979–7008. [CrossRef]
112. Wolfer, W.G. Elastic properties of surfaces on nanoparticles. *Acta Mater.* **2011**, *59*, 7736–7743. [CrossRef]
113. Khater, M.E.; Eltaher, M.A.; Abdel-Rahman, E.; Yavuz, M. Surface and thermal load effects on the buckling of curved nanowires. *Eng. Sci. Technol. Int. J.* **2014**, *17*, 279–283. [CrossRef]
114. Wang, J.; Xiao, J. Analytical solutions of bending analysis and vibration of rectangular nano laminates with surface effects. *Appl. Math. Model.* **2022**, *110*, 663–673. [CrossRef]
115. Allahyari, E.; Fadaee, M. Analytical investigation on free vibration of circular double-layer graphene sheets including geometrical defect and surface effects. *Compos. Part B Eng.* **2016**, *85*, 259–267. [CrossRef]
116. Sadeghian, M.; Palevicius, A.; Janusas, G. Nonlinear Thermal/Mechanical Buckling of Orthotropic Annular/Circular Nanoplate with the Nonlocal Strain Gradient Model. *Micromachines* **2023**, *14*, 1790. [CrossRef]
117. Ebrahimi, F.; Dabbagh, A. Application of the nonlocal strain gradient elasticity on the wave dispersion behaviors of inhomogeneous nanosize beams. *Eur. Phys. J. Plus* **2019**, *134*, 112. [CrossRef]
118. Liu, X.; Bie, Z.; Yu, P.; Zheng, B.; Shi, X.; Fan, Y.; He, X.; Lu, C. Peridynamics for the fracture study on multi-layer graphene sheets. *Compos. Struct.* **2024**, *332*, 117926. [CrossRef]
119. Izadi, R.; Das, R.; Fantuzzi, N.; Trovalusci, P. Fracture properties of green nano fibrous network with random and aligned fiber distribution: A hierarchical molecular dynamics and peridynamics approach. *Int. J. Eng. Sci.* **2024**, *204*, 104136. [CrossRef]
120. Thai, C.H.; Fereira, A.M.J.; Nguyen-Xuan, H.; Hung, P.T.; Phung-Van, P. A nonlocal strain gradient isogeometric model for free vibration analysis of magneto-electro-elastic functionally graded nanoplates. *Compos. Struct.* **2023**, *316*, 117005. [CrossRef]
121. Rajasekaran, S. Numerical investigation of non-local elasticity theory for free vibration of polymer embedded multi-layer graphene sheets. *Mater. Today Commun.* **2024**, *39*, 108669. [CrossRef]
122. Orlandini, G.; Turro, F. Integral Transform Methods: A Critical Review of Various Kernels. *Few-Body Syst.* **2017**, *58*, 76. [CrossRef]
123. Moreno-García, P.; dos Santos, J.V.A.; Lopes, H. A Review and Study on Ritz Method Admissible Functions with Emphasis on Buckling and Free Vibration of Isotropic and Anisotropic Beams and Plates. *Arch. Comput. Methods Eng.* **2018**, *25*, 785–815. [CrossRef]
124. Zhou, P.-B. Finite difference method. In *Numerical Analysis of Electromagnetic Fields*; Zhou, P.-B., Ed.; Springer: Berlin/Heidelberg, Germany, 1993; pp. 63–94.
125. Wu, T.Y.; Liu, G.R. A Differential Quadrature as a numerical method to solve differential equations. *Comput. Mech.* **1999**, *24*, 197–205. [CrossRef]
126. Shu, C. Application of differential quadrature method to structural and vibration analysis. In *Differential Quadrature and Its Application in Engineering*; Shu, C., Ed.; Springer: London, UK, 2000; pp. 186–223.
127. Palacz, M. Spectral Methods for Modelling of Wave Propagation in Structures in Terms of Damage Detection—A Review. *Appl. Sci.* **2018**, *8*, 1124. [CrossRef]

128. Hesthaven, J.S. Spectral methods for hyperbolic problems. This revised and updated chapter is based partly on work from the author's original article first published in the Journal of computational and applied mathematics, Volume 128, Gottlieb and Hesthaven, Elsevier, 2001. In *Handbook of Numerical Analysis*; Abgrall, R., Shu, C.-W., Eds.; Elsevier: Amsterdam, The Netherlands, 2016; Chapter 17; Volume 17, pp. 441–466.
129. Gabbasov, R.; Filatov, V.; Dao, N.K.; Quyen Hoang, T.L. Analysis of bending plates with mixed boundary conditions using generalized equations of finite difference method. *IOP Conf. Ser. Mater. Sci. Eng.* **2020**, *913*, 022018. [CrossRef]
130. Jankowski, J.; Kotełko, M.; Ungureanu, V. Numerical and Experimental Analysis of Buckling and Post-Buckling Behaviour of TWCFS Lipped Channel Section Members Subjected to Eccentric Compression. *Materials* **2024**, *17*, 2874. [CrossRef] [PubMed]
131. Zhang, H.; Wang, C.M.; Challamel, N. Modelling vibrating nano-strings by lattice, finite difference and Eringen's nonlocal models. *J. Sound Vib.* **2018**, *425*, 41–52. [CrossRef]
132. Monge, J.C.; Mantari, J.L. 3D nonlocal solution with layerwise approach and DQM for multilayered functionally graded shallow nanoshells. *Mech. Adv. Mater. Struct.* **2025**, *32*, 1352–1362. [CrossRef]
133. Al Mukahal, F.H.H.; Sobhy, M.; Al-Ali, A.H.K. Magneto-Hygrothermal Deformation of FG Nanocomposite Annular Sandwich Nanoplates with Porous Core Using the DQM. *Crystals* **2025**, *15*, 827. [CrossRef]
134. Tepe, A. Vibration analysis of SWCNTs resting on an elastic foundation using the initial values method. *J. Eng. Math.* **2025**, *152*, 20. [CrossRef]
135. Monge, J.C.; Mantari, J.L. Semi-analytical layerwise solutions for FG MEE complex shell structures. *Eur. J. Mech. A/Solids* **2025**, *109*, 105446. [CrossRef]
136. Li, C.; Wei, P.; Guo, X. The spectral methods for the propagation of thermoelastic waves in multilayer cylinders based on nonlocal strain gradient elasticity. *Acta Mech.* **2024**. [CrossRef]
137. Yi, X.; Li, B.; Wang, Z. Vibration Analysis of Fluid Conveying Carbon Nanotubes Based on Nonlocal Timoshenko Beam Theory by Spectral Element Method. *Nanomaterials* **2019**, *9*, 1780. [CrossRef]
138. Jalali, S.K.; Heshmati, M. Buckling analysis of circular sandwich plates with tapered cores and functionally graded carbon nanotubes-reinforced composite face sheets. *Thin-Walled Struct.* **2016**, *100*, 14–24. [CrossRef]
139. Oden, J.T.; Reddy, J.N. Variational principles in continuum mechanics. In *Variational Methods in Theoretical Mechanics*; Oden, J.T., Reddy, J.N., Eds.; Springer: Berlin/Heidelberg, Germany, 1976; pp. 139–214.
140. Agrawal, V.; Gautam, S.S. IGA: A Simplified Introduction and Implementation Details for Finite Element Users. *J. Inst. Eng. Ser. C* **2019**, *100*, 561–585. [CrossRef]
141. Anjomshoa, A.; Tahani, M. Vibration analysis of orthotropic circular and elliptical nano-plates embedded in elastic medium based on nonlocal Mindlin plate theory and using Galerkin method. *J. Mech. Sci. Technol.* **2016**, *30*, 2463–2474. [CrossRef]
142. Liu, X.; He, X.; Lu, C.; Oterkus, E. Peridynamic modeling at nano-scale. In *Peridynamic Modeling, Numerical Techniques, and Applications*; Oterkus, E., Oterkus, S., Madenci, E., Eds.; Elsevier: Amsterdam, The Netherlands, 2021; Chapter 16; pp. 355–370.
143. Li, S.; Urata, S. An atomistic-to-continuum molecular dynamics: Theory, algorithm, and applications. *Comput. Methods Appl. Mech. Eng.* **2016**, *306*, 452–478. [CrossRef]
144. Boichuk, O.; Chuiko, S.; Diachenko, D.y. Adomian's Decomposition Method in the Theory of Nonlinear Autonomous Boundary-Value Problems. *Ukr. Math. J.* **2024**, *75*, 1203–1218. [CrossRef]
145. Mohamed, S.A.; Shanab, R.A.; Seddek, L.F. Vibration analysis of Euler–Bernoulli nanobeams embedded in an elastic medium by a sixth-order compact finite difference method. *Appl. Math. Model.* **2016**, *40*, 2396–2406. [CrossRef]
146. Tian, Z.F.; Yu, P.X. An efficient compact difference scheme for solving the streamfunction formulation of the incompressible Navier–Stokes equations. *J. Comput. Phys.* **2011**, *230*, 6404–6419. [CrossRef]
147. Karami, B.; Janghorban, M.; Dimitri, R.; Tornabene, F. Free Vibration Analysis of Triclinic Nanobeams Based on the Differential Quadrature Method. *Appl. Sci.* **2019**, *9*, 3517. [CrossRef]
148. Jena, S.K.; Chakraverty, S.; Tornabene, F. Buckling Behavior of Nanobeams Placed in Electromagnetic Field Using Shifted Chebyshev Polynomials-Based Rayleigh-Ritz Method. *Nanomaterials* **2019**, *9*, 1326. [CrossRef]
149. Torkashvand, Z.; Shayeganfar, F.; Ramazani, A. Nanomaterials Based Micro/Nanoelectromechanical System (MEMS and NEMS) Devices. *Micromachines* **2024**, *15*, 175. [CrossRef] [PubMed]
150. Pruchnik, B.; Kwoka, K.; Piasecki, T.; Ghourichaei, M.J.; Kerimzade, U.; Aydin, O.; Aksoy, B.; Aydogan, C.; Nadar, G.; Rangelow, I.W.; et al. Characterization of a hybrid nanowire-MEMS force sensor using direct actuation. *Meas. Sci. Technol.* **2025**, *36*, 075024. [CrossRef]
151. Xiao, Y.; Luo, F.; Zhang, Y.; Hu, F.; Zhu, M.; Qin, S. A Review on Graphene-Based Nano-Electromechanical Resonators: Fabrication, Performance, and Applications. *Micromachines* **2022**, *13*, 215. [CrossRef]
152. Ke, T.V.; Minh, P.V.; Thom, D.V.; Duc, N.D. Static and dynamic analysis of doubly-curved functionally graded porous nanoshells integrated with piezoelectric surface layers and flexoelectric effect. *Comput. Struct.* **2025**, *312*, 107737. [CrossRef]

153. Omar, I.; Marhoon, T.; Babadoust, S.; Najm, A.S.; Pirmoradian, M.; Salahshour, S.; Sajadi, S.M. Static stability of functionally graded porous nanoplates under uniform and non-uniform in-plane loads and various boundary conditions based on the nonlocal strain gradient theory. *Results Eng.* **2025**, *25*, 103612. [CrossRef]
154. Brischetto, S.; Cesare, D. A 3D shell model for static and free vibration analysis of multilayered magneto-elastic structures. *Thin-Walled Struct.* **2025**, *206*, 112620. [CrossRef]
155. Anh, V.T.T.; Dat, N.D.; Nguyen, P.D.; Duc, N.D. A nonlocal higher-order shear deformation approach for nonline ar static analysis of magneto-electro-elastic sandwich Micro/Nano-plates with FG-CNT core in hygrothermal environment. *Aerosp. Sci. Technol.* **2024**, *147*, 109069. [CrossRef]
156. Genel, Ö.E.; Koç, H.; Tüfekci, E. In-Plane Static Analysis of Curved Nanobeams Using Exact-Solution-Based Finite Element Formulation. *Comput. Mater. Contin.* **2025**, *82*, 2043–2059. [CrossRef]
157. Wu, J.; Song, L.; Huang, K. Nonlinear static behaviors of nonlocal nanobeams incorporating longitudinal linear temperature gradient. *Int. J. Therm. Sci.* **2025**, *208*, 109421. [CrossRef]
158. Behnam-Rasouli, M.-S.; Challamel, N.; Karamodin, A.; Sani, A.A. Application of the Green's function method for static analysis of nonlocal stress-driven and strain gradient elastic nanobeams. *Int. J. Solids Struct.* **2024**, *295*, 112794. [CrossRef]
159. Zheng, Y.-F.; Qu, D.-Y.; Liu, L.-C.; Chen, C.-P. Size-dependent nonlinear bending analysis of nonlocal magneto-electro-elastic laminated nanobeams resting on elastic foundation. *Int. J. Non-Linear Mech.* **2023**, *148*, 104255. [CrossRef]
160. Soltani, M.; Momenian, M.H.; Civalek, O. Stability analysis of sandwich double nanobeam-system with varying cross-section interconnected by Kerr-type three-parameter elastic layer. *Thin-Walled Struct.* **2024**, *204*, 112249. [CrossRef]
161. Ren, Y.; Qing, H. Bending and buckling analysis of functionally graded Timoshenko nanobeam using Two-Phase Local/Nonlocal piezoelectric integral model. *Compos. Struct.* **2022**, *300*, 116129. [CrossRef]
162. Barretta, R.; Luciano, R.; Marotti de Sciarra, F.; Vaccaro, M.S. On torsion of FG elastic nanobeams on nonlocal foundations. *Compos. Struct.* **2024**, *340*, 118146. [CrossRef]
163. Alghanmi, R.A. Size-dependent static response of a functionally graded nanobeam attached to a piezoelectric fibre-reinforced composite actuator. *Sci. Rep.* **2025**, *15*, 28734. [CrossRef] [PubMed]
164. Tuna, M.; Kirca, M. Exact solution of Eringen's nonlocal integral model for bending of Euler–Bernoulli and Timoshenko beams. *Int. J. Eng. Sci.* **2016**, *105*, 80–92. [CrossRef]
165. Ma, W.; Li, X. A higher-order beam theory for analyzing the static and dynamic behaviors of box and tubular beam-columns with the higher-order effect of axial force. *Acta Mech. Sin.* **2025**, *42*, 524391. [CrossRef]
166. Tuyen, B.V.; Du, N.D. Analytic solutions for static bending and free vibration analysis of FG nanobeams in thermal environment. *J. Therm. Stress.* **2023**, *46*, 871–894. [CrossRef]
167. Zhaowei, Z.; Zhiqiang, S.; Aiyun, L.; Habibi, M.; Albaijan, I.; Zhang, D. Static responses for Graphene nanoplatlet reinforced aerobic sport plate. *Adv. Nano Res.* **2025**, *18*, 565.
168. Hoai, L.; Trai, V.K.; Tran, V.K.; Nguyen Thi Thu, H. Static and dynamic response of bidirectional functionally graded porous nanoplate taking into account surface effect using isogeometric approach. *Mech. Based Des. Struct. Mach.* **2025**, 1–44. [CrossRef]
169. Van Thom, D.; Chinh, V.M.; Van Minh, P.; Anh Vu, N.D. Mechanical responses of nanoplates resting on viscoelastic foundations in multi-physical environments. *Eur. J. Mech. A/Solids* **2024**, *106*, 105309. [CrossRef]
170. Altekin, M.; Karatas, E.E.; Yükseler, R.F. Stress-driven nonlocal theory on nonlinear static analysis of annular nanoplates. *Mech. Based Des. Struct. Mach.* **2025**, *53*, 6283–6328. [CrossRef]
171. Jafarinezhad, M.; Sburlati, R.; Cianci, R. Static and free vibration analysis of functionally graded annular plates using stress-driven nonlocal theory. *Eur. J. Mech. A/Solids* **2023**, *99*, 104955. [CrossRef]
172. Tho, N.C.; Tien, D.M.; Thom, D.V.; Minh, P.V.; Doan, D.V. A new approach to the static bending problem of organic nanoplates. *Proc. Inst. Mech. Eng. Part C J. Mech. Eng. Sci.* **2025**, *239*, 3052–3064. [CrossRef]
173. Tang, F.; He, S.; Shi, S.; Dong, F.; Xiao, X.; Liu, S. Mechanical behavior of nanocircular plates under coupled surface and nonlocal effects by using molecular dynamics simulations. *Phys. Lett. A* **2024**, *500*, 129380. [CrossRef]
174. Bab, Y.; Dorduncu, M.; Kutlu, A.; Markert, B. Nonlocal static modeling of laminated composite shells using peridynamic differential operator in a higher-order shear deformation framework. *Eng. Anal. Bound. Elem.* **2025**, *179*, 106384. [CrossRef]
175. Reddy, J.N.; Liu, C. *A Higher-Order Theory for Geometrically Nonlinear Analysis of Composite Laminates*; NASA: Washington, DC, USA, 1987.
176. Guo, Y.; Alam, M. Nonlinear bending and thermal postbuckling of magneto-electro-elastic nonlocal strain-gradient beam including surface effects. *Appl. Math. Model.* **2025**, *142*, 115955. [CrossRef]
177. Van Lieu, P. Thermal buckling of organic nanobeams resting on viscous elastic foundation. *Eur. J. Mech. A/Solids* **2025**, *109*, 105455. [CrossRef]
178. Sahmani, S.; Kotrasova, K.; Zareichian, M.; Sun, J.; Safaei, B. Nonlinear asymmetric thermomechanical buckling of shallow nanoscale arches having dissimilar end conditions embracing nonlocality and strain gradient size dependencies. *Def. Technol.* **2025**, *47*, 67–82. [CrossRef]

179. Zhang, J.; Chen, P.; Peng, J.; Liu, H.; Peng, G.; Zhang, Y. Buckling instability of graphyne nanosheets under local indentation. *Mech. Mater.* **2025**, *200*, 105206. [CrossRef]
180. Hou, G.; Al-Mussawi, W.; Khidhir, D.M.; Singh, N.S.S.; Saeidlou, S.; Al-Bahrani, M.; Salahshour, S.; Sajadi, S.M.; Hasanabad, A.M. Investigating the effect of variable heat flux on buckling of carbon nanotube using non-equilibrium molecular dynamic simulation. *Int. Commun. Heat Mass Transf.* **2025**, *167*, 109300. [CrossRef]
181. Yang, F.; Deng, Y.; Wang, J.; Huo, J.; Zhang, T. Post buckling behavior of porous magneto-electro-elastic nanoplates using nonlocal strain gradient theory. *Results Eng.* **2025**, *27*, 106446. [CrossRef]
182. Sahmani, S.; Rabczuk, T.; Song, J.-H.; Safaei, B. Unified nonlocal surface elastic-based thermal induced asymmetric nonlinear buckling of inhomogeneous nano-arches subjected to dissimilar end conditions. *Compos. Struct.* **2025**, *357*, 118961. [CrossRef]
183. Tekin Atacan, A.; Yükseler, R.F. Size-dependent snap buckling behavior of functionally graded sinusoidal shallow nano-arches supported by elastic horizontal springs using the stress-driven nonlocal approach. *Mech. Res. Commun.* **2025**, *148*, 104487. [CrossRef]
184. Van Lieu, P.; Zenkour, A.M.; Luu, G.T. Static bending and buckling of FG sandwich nanobeams with auxetic honeycomb core. *Eur. J. Mech. A/Solids* **2024**, *103*, 105181. [CrossRef]
185. Tang, Y.; Bian, P.-L.; Qing, H. Buckling and vibration analysis of axially functionally graded nanobeam based on local stress- and strain-driven two-phase local/nonlocal integral models. *Thin-Walled Struct.* **2024**, *202*, 112162. [CrossRef]
186. Georgantzinos, S.K.; Antoniou, P.A.; Stamoulis, K.P.; Spitas, C. Influence of microstructural and environmental factors on the buckling performance of carbon nanotube-enhanced laminated composites: A multiscale analysis. *Eng. Fail. Anal.* **2024**, *158*, 108055. [CrossRef]
187. Hafed, Z.S. Effects of new nonlinear curvature models and non-local elasticity on buckling investigation of FG tapered nano-beams locating on elastic foundations. *J. Eng. Res.* **2024**. [CrossRef]
188. Sahmani, S.; Safaei, B.; Rabczuk, T. On the Role of Nonlocal Strain Gradient Elasticity in Nonlinear Buckling of FG Porous Reinforced Curved Nanobeams Having Different Degrees of Curvature. *Int. J. Struct. Stab. Dyn.* **2024**, *25*, 2550134. [CrossRef]
189. Dang Van, H.; Nguyen Thi, H.; Nguyen Thi Kim, T. Size-dependent buckling analysis of functionally graded carbon nanotubes-reinforced composite nano-plates based on nonlocal strain gradient theory. *Struct. Eng. Mech.* **2025**, *94*, 335–350. [CrossRef]
190. Buğday, M.; Kafalı, A.; Esen, İ. Effect of the honeycomb structure on the thermo mechanical buckling of sandwich nanoplates exposed to magnetic and thermal fields. *Mech. Adv. Mater. Struct.* **2025**, 1–22. [CrossRef]
191. Wang, J.; Xiao, J.; Xia, X. Buckling and post-buckling behavior of nano-laminates considering surface effects. *Arch. Appl. Mech.* **2024**, *94*, 3469–3488. [CrossRef]
192. Yıldız, T. Comprehensive study on the determination of thermal buckling of functionally graded nano sandwich plates with auxetic butterfly cores. *Mech. Based Des. Struct. Mach.* **2025**, 1–25. [CrossRef]
193. Penna, R.; Lovisi, G.; Feo, L. Buckling analysis of functionally graded nanobeams via surface stress-driven model. *Int. J. Eng. Sci.* **2024**, *205*, 104148. [CrossRef]
194. Sofiyev, A.H.; Avey, M.; Aslanova, N.M. A Mathematical Approach to the Buckling Problem of Axially Loaded Laminated Nanocomposite Cylindrical Shells in Various Environments. *Math. Comput. Appl.* **2025**, *30*, 10. [CrossRef]
195. Gui, Y.; Wu, R. A novel buckling model for layered cylindrical nanoshells incorporates interfacial effect. *Appl. Math. Model.* **2026**, *150*, 116417. [CrossRef]
196. Gholami, R.; Ansari, R.; Aghdasi, P.; Sahmani, S. Buckling and postbuckling of embedded sandwich moderately thick plates with functionally graded graphene nanoplatelet-reinforced porous core and metallic face sheets. *Thin-Walled Struct.* **2025**, *210*, 113063. [CrossRef]
197. Salari, E.; Sadough Vanini, S.A. Nonlocal nonlinear static/dynamic snap-through buckling and vibration of thermally post-buckled imperfect functionally graded circular nanoplates. *Waves Random Complex Media* **2025**, *35*, 3805–3851. [CrossRef]
198. Li, Q.; Zhao, X.; Pan, Z.; Zhang, J. Nonlinear post-buckling of graded porous circular nanoplate with surface stress subjected to follower force. *Mech. Adv. Mater. Struct.* **2025**, *32*, 341–354. [CrossRef]
199. Atacan, A.T.; Yükseler, R.F. Nonlinear buckling and post-buckling analyses of functionally graded circular shallow arches. *Proc. Inst. Mech. Eng. Part C J. Mech. Eng. Sci.* **2023**, *238*, 4768–4789. [CrossRef]
200. Songsuwan, W.; Thai, S.; Wattanasakulpong, N. Buckling and post-buckling behavior of ideal and non-ideal FG-GPLRC beams in thermal environment. *Acta Mech. Sin.* **2024**, *41*, 424374. [CrossRef]
201. Sajjadi, M.S.; Shaterzadeh, A.R. Thermal and mechanical post-buckling analysis of the composite truncated conical shells reinforced with the lattice core. *Acta Mech.* **2025**. [CrossRef]
202. Bochkarev, A. Buckling of a nano-rod with taken into account of surface effect. *Z. Für Angew. Math. Mech.* **2024**, *104*, e202300738. [CrossRef]
203. Wang, W.; Qi, Q.; Zhang, J.; Wang, Z.; Sun, J.; Zhou, Z.; Xu, X. A size-dependent electro-mechanical buckling analysis of flexoelectric cylindrical nanoshells. *Thin-Walled Struct.* **2024**, *202*, 112118. [CrossRef]

204. Ozdemir, M.T.; Das, T.; Esen, I. Effect of the hexachiral auxetic structure on the thermal buckling behaviour of the magneto electro elastic sandwich smart nano plate using nonlocal strain gradient elasticity. *Int. J. Mech. Mater. Des.* **2025**, 130. [CrossRef]
205. Ebrahimi, F.; Barati, M.R. Buckling analysis of nonlocal strain gradient axially functionally graded nanobeams resting on variable elastic medium. *Proc. Inst. Mech. Eng. Part C J. Mech. Eng. Sci.* **2017**, *232*, 2067–2078. [CrossRef]
206. Li, L.; Hu, Y. Post-buckling analysis of functionally graded nanobeams incorporating nonlocal stress and microstructure-dependent strain gradient effects. *Int. J. Mech. Sci.* **2017**, *120*, 159–170. [CrossRef]
207. Khaniki, H.B.; Hosseini-Hashemi, S. Buckling analysis of tapered nanobeams using nonlocal strain gradient theory and a generalized differential quadrature method. *Mater. Res. Express* **2017**, *4*, 065003. [CrossRef]
208. Zhang, B.; Shen, H.; Liu, J.; Wang, Y.; Zhang, Y. Deep postbuckling and nonlinear bending behaviors of nanobeams with nonlocal and strain gradient effects. *Appl. Math. Mech.* **2019**, *40*, 515–548. [CrossRef]
209. Bochkarev, A.O.; Grekov, M.A. Influence of Surface Stresses on the Nanoplate Stiffness and Stability in the Kirsch Problem. *Phys. Mesomech.* **2019**, *22*, 209–223. [CrossRef]
210. Grekov, M.A.; Bochkarev, A.O. Buckling of a stretched nanoplate with a nanohole incorporating surface energy. *Int. J. Eng. Sci.* **2024**, *199*, 104075. [CrossRef]
211. Wang, A.; Li, J. Surface effects on buckling of nanotubes under uniaxial compression. *Mater. Lett.* **2025**, *387*, 138196. [CrossRef]
212. Alrubea, N.A.; Abouelregal, A.E. Thermoelastic dynamics of viscoelastic nanobeams on elastic foundations under multi-physics interactions. *Results Eng.* **2025**, *27*, 106154. [CrossRef]
213. Sur, A.; Mondal, S.; Das, S. Size-dependent vibrations of piezo-thermoelastic microbeam using dual-scale nonlocal strain gradient and memory-dependent thermoelasticity theories. *Contin. Mech. Thermodyn.* **2025**, *37*, 78. [CrossRef]
214. Ren, Y.-M.; Qing, H. Size-dependent buckling and vibration of functionally graded magneto-electro-thermo-elastic Timoshenko nanobeams using general stress-driven two-phase local/nonlocal integral model. *Thin-Walled Struct.* **2025**, *215*, 113480. [CrossRef]
215. Das, B.; Ussorio, D.; Vaccaro, M.S.; Barretta, R.; Luciano, R. Dynamics of FG nanobeams on nonlocal medium. *Compos. Struct.* **2025**, *366*, 119057. [CrossRef]
216. Koç, M.A.; Esen, İ.; Eroğlu, M. Thermal and Mechanical Vibration Response of Auxetic Core Sandwich Smart Nanoplate. *Adv. Eng. Mater.* **2024**, *26*, 2400797. [CrossRef]
217. Zou, Y.; Kiani, Y. Vibrations of Nonlocal Polymer-GPL Plates at Nanoscale: Application of a Quasi-3D Plate Model. *Mathematics* **2023**, *11*, 4109. [CrossRef]
218. Cuong-Le, T.; Le, M.H.; Linh-Nguyen, T.T.; Luong, V.H.; Khatir, S.; Tran, M.T.; Nguyen, T.-B. A Nonlocal Numerical Solution Based on Carrera Unified Formulation for Static and Free Vibration Analysis of Laminated Composite Nanoplate. *Int. J. Struct. Stab. Dyn.* **2024**, *25*, 2550060. [CrossRef]
219. Hoan, P.V.; Anh, N.D.; Thom, D.V.; Minh, P.V. Nonlinear vibration of nanobeams in thermal environment. *Mech. Based Des. Struct. Mach.* **2025**, *53*, 5690–5716. [CrossRef]
220. Binh, V.H.; Anh, N.D.; Van Thom, D.; Minh, P.V.; Dung, H.T. Vibration response of nanobeams subjected to random reactions. *Eur. J. Mech. A/Solids* **2025**, *109*, 105489. [CrossRef]
221. Ahmad, H.; Abouelregal, A.E.; Benhamed, M.; Alotaibi, M.F.; Jendoubi, A. Vibration analysis of nanobeams subjected to gradient-type heating due to a static magnetic field under the theory of nonlocal elasticity. *Sci. Rep.* **2022**, *12*, 1894. [CrossRef] [PubMed]
222. Herisanu, N.; Marinca, B.; Marinca, V. Longitudinal–Transverse Vibration of a Functionally Graded Nanobeam Subjected to Mechanical Impact and Electromagnetic Actuation. *Symmetry* **2023**, *15*, 1376. [CrossRef]
223. Zhang, J.; Yang, Y. Vibration of piezoelectric nanobeams with flexoelectric effect carrying an attached mass. *Acta Mech.* **2025**. [CrossRef]
224. Uzun, B.; Kafkas, U.; Yaylı, M.Ö.; Güçlü, G. Torsional vibration behavior of a restrained non-circular nanowire in an elastic matrix. *Mech. Based Des. Struct. Mach.* **2024**, *52*, 8216–8248. [CrossRef]
225. Kadıoğlu, H.G.; Yaylı, M.Ö. Analysis of torsional vibration in viscoelastic functionally graded nanotubes with viscoelastic constraints using doublet mechanics theory. *Int. J. Mech. Mater. Des.* **2025**, 1–23. [CrossRef]
226. Kadioglu, H.G.; Uzun, B.; Yayli, M.O. Size-dependent vibration analysis of a FG viscoelastic nanotube attached with the time-dependent boundary conditions using NLSGT. *Z. Für Angew. Math. Und Mech.* **2025**, *105*, e202400934. [CrossRef]
227. Akpınar, M.; Kafkas, U.; Uzun, B.; Yaylı, M.Ö. On the torsional vibration of a porous nanorod with arbitrary boundary conditions considering nonlocal lam strain gradient theory. *Eur. J. Mech. A/Solids* **2025**, *111*, 105610. [CrossRef]
228. Li, Y.; Han, Y.; Gao, J.; Li, M. Investigation on torsional dynamic behavior of imperfect multi-walled carbon nanotube-strengthened nanocomposite beams. *Mech. Based Des. Struct. Mach.* **2025**, *53*, 4620–4635. [CrossRef]
229. Uzun, B.; Yaylı, M.Ö.; Civalek, Ö. An investigation on the torsional vibration of a FG strain gradient nanotube. . *Für Angew. Math. Und Mech.* **2024**, *104*, e202301093. [CrossRef]
230. Welles, N.W.; Ma, M.; Ekinci, K.; Paul, M.R. Theoretical modeling of the dynamic range of an elastic nanobeam under tension with a geometric nonlinearity. *J. Appl. Phys.* **2025**, *138*. [CrossRef]

231. Huang, Y.; Huang, R.; Zhang, J. Dynamic Stability of Nanobeams Based on the Reddy's Beam Theory. *Materials* **2023**, *16*, 1626. [CrossRef] [PubMed]
232. Mohammed, D.A.; Hussein, N.A. Nonlinear Nonlocal Torsional Vibration Analysis of Temperature-Dependent Viscoelastic Carbon Nanotubes Embedded in a Viscoelastic Medium Using Kelvin-Voigt Model. *J. Vib. Eng. Technol.* **2025**, *13*, 303. [CrossRef]
233. Jayan, M.M.S.; Wang, L.; Selvamani, R.; Ramya, N. Analysis of Vibrational Properties of Horn-Shaped Magneto-Elastic Single-Walled Carbon Nanotube Mass Sensor Conveying Pulsating Viscous Fluid Using Haar Wavelet Technique. *Acta Mech. Solida Sin.* **2024**, *37*, 685–699. [CrossRef]
234. Akpınar, M.; Uzun, B.; Kadıoğlu, H.G.; Yaylı, M.Ö. Dynamic analysis of restrained short-fiber-reinforced and functionally graded nanobeams via stress-driven model. *Z. Für Angew. Math. Mech.* **2025**, *105*, e70133. [CrossRef]
235. Kafali, A.; Kartaltepe, O.; Esen, İ. Vibration analysis of smart sandwich nanoplate incorporating butterfly auxetic core and piezoelectric face layers under thermal field. *Acta Mech.* **2025**, *236*, 3515–3541. [CrossRef]
236. Wang, A.; Zhang, K. Free Vibration of Graphene Nanoplatelet-Reinforced Porous Double-Curved Shells of Revolution with a General Radius of Curvature Based on a Semi-Analytical Method. *Mathematics* **2024**, *12*, 3060. [CrossRef]
237. Fang, K.; Huang, G.; Yu, G.; Xu, W.; Yuan, W. Free vibration analysis of graphene origami-reinforced nano cylindrical shell. *Mech. Adv. Mater. Struct.* **2024**, *31*, 12099–12111. [CrossRef]
238. Numanoğlu, H.M.; Civalek, Ö. On shear-dependent vibration of nano frames. *Int. J. Eng. Sci.* **2024**, *195*, 103992. [CrossRef]
239. Tran, L.V.; Tran, D.B.; Phan, P.T.T. Free vibration analysis of stepped FGM nanobeams using nonlocal dynamic stiffness model. *J. Low Freq. Noise Vib. Act. Control* **2023**, *42*, 997–1017. [CrossRef]
240. Wang, P.; Xu, J.; Zhang, X.; Lv, Y. Free vibration of nanobeams with surface and dynamic flexoelectric effects. *Sci. Rep.* **2024**, *14*, 30192. [CrossRef]
241. Natsuki, J.; Lei, X.-W.; Wu, S.; Natsuki, T. Modeling and Vibration Analysis of Carbon Nanotubes as Nanomechanical Resonators for Force Sensing. *Micromachines* **2024**, *15*, 1134. [CrossRef]
242. Karamanli, A.; Nguyen, N.-D.; Lee, S.; Vo, T.P. Improved FSDT for forced vibration analysis of nanobeams under moving concentrated loads via doublet mechanics. *Mech. Based Des. Struct. Mach.* **2025**, 1–24. [CrossRef]
243. Padhiyar, M.; Karsh, P.K.; Bandhania, G.K. Deterministic and stochastic free vibration analysis of CNT reinforced functionally graded cantilever plates. *Sci. Rep.* **2025**, *15*, 31761. [CrossRef] [PubMed]
244. Jankowski, P.; Żur, K.K. Steady-state vibration of nanocomposite structures with discontinuities. *Aerosp. Sci. Technol.* **2026**, *168*, 110885. [CrossRef]
245. Uzun, B.; Yaylı, M.Ö. Free Vibration of a Carbon Nanotube-Reinforced Nanowire/Nanobeam with Movable Ends. *J. Vib. Eng. Technol.* **2024**, *12*, 6847–6863. [CrossRef]
246. Alizadeh, A.; Shishehsaz, M.; Shahrooi, S.; Reza, A. Free vibration characteristics of viscoelastic nano-disks based on modified couple stress theory. *J. Strain Anal. Eng. Des.* **2022**, *58*, 270–296. [CrossRef]
247. Dinh, T.B.; Van Lien, T. Free vibration analysis of multiple-cracked functionally graded nanostructures. *Acta Mech.* **2025**. [CrossRef]
248. Tang, Y.; Bian, P.-L.; Qing, H. Isogeometric analysis for free vibration of axially functionally graded Timoshenko nanobeams based on stress-driven local/nonlocal models. *Mech. Based Des. Struct. Mach.* **2025**, 1–24. [CrossRef]
249. Feo, L.; Lovisi, G.; Penna, R. Free vibration analysis of functionally graded nanobeams based on surface stress-driven nonlocal model. *Mech. Adv. Mater. Struct.* **2024**, *31*, 10391–10399. [CrossRef]
250. Abasi, M.; Hosseini, S.A. Exact solution for force vibration of Timoshenko nanobeam via acceleration moving load. *Mech. Based Des. Struct. Mach.* **2025**, 1–23. [CrossRef]
251. Zhao, T.Y.; Wang, Y.X.; Chen, L. Mathematical modeling and vibration analysis of rotating functionally graded porous spacecraft systems reinforced by graphene nanoplatelets. *Math. Methods Appl. Sci.* **2025**, *48*, 7514–7538. [CrossRef]
252. Hoai Nam, V.; Tien Tu, B.; Van Doan, C.; Nhu Nam, P.; Minh Duc, V. A new semi-analytical approach for nonlinear dynamic responses of functionally graded porous graphene platelet-reinforced circular plates and spherical shells. *Proc. Inst. Mech. Eng. Part C J. Mech. Eng. Sci.* **2024**, *239*, 730–742. [CrossRef]
253. Atanasov, M.S.; Pavlović, I.R.; Simonović, J.; Borzan, C.; Păcurar, A.; Păcurar, R. Forced Dynamics of Elastically Connected Nano-Plates and Nano-Shells in Winkler-Type Elastic Medium. *Appl. Sci.* **2025**, *15*, 2765. [CrossRef]
254. Tariq, A.; Uzun, B.; Deliktaş, B.; Yaylı, M.Ö. Application of machine learning methodology for investigating the vibration behavior of functionally graded porous nanobeams. *J. Strain Anal. Eng. Des.* **2024**, *60*, 131–151. [CrossRef]
255. Kumar, R.; Kumar, A.; Ranjan Kumar, D. Buckling response of CNT based hybrid FG plates using finite element method and machine learning method. *Compos. Struct.* **2023**, *319*, 117204. [CrossRef]
256. Mazari, M.Y.; Hamza, B.; Dehbi, F.; Cheikh, A.; Saimi, A.; Bensaid, I. Hybrid Galerkin-machine learning approach for dynamic analysis of nanocomposite beams under thermal effects. *Mech. Based Des. Struct. Mach.* **2025**, 1–18. [CrossRef]
257. Lal, H.P.; Abhiram, B.R.; Ghosh, D. Prediction of nonlocal elasticity parameters using high-throughput molecular dynamics simulations and machine learning. *Eur. J. Mech. A/Solids* **2024**, *103*, 105175. [CrossRef]

258. Orts Mercadillo, V.; Ijije, H.; Chaplin, L.; Kinloch, I.A.; Bissett, M.A. Novel techniques for characterising graphene nanoplatelets using Raman spectroscopy and machine learning. *2D Mater.* **2023**, *10*, 025018. [CrossRef]
259. Yan, C.A.; Vescovini, R.; Fantuzzi, N. A neural network-based approach for bending analysis of strain gradient nanoplates. *Eng. Anal. Bound. Elem.* **2023**, *146*, 517–530. [CrossRef]